



Investigation of structural and magnetic properties of rare earth doped Co-Ferrite nanoparticles using X ray powder diffraction, Mossbauer effect spectroscopy and neutron diffraction measurements.

Mohammed Yehia Elbahrawy

Professor – Nuclear Solid State Physics

Egyptian Atomic Energy Authority



Investigation of structural and magnetic properties of rare earth doped Co-Ferrite nanoparticles using X ray powder diffraction, Mossbauer effect spectroscopy and neutron diffraction measurements.



Institute of Physics and Technology,
Mongolian Academy of Sciences

M. Yehia
A. Hashhash
M. Kaiser

I. Bobrikov

E. Uyanga



Outline

1

Introduction

- Magnetism
- Ferrites

2

Experimental

- Preparation
- Techniques

3

$\text{CoFe}_{2-x}\text{Ce}_x\text{O}_4$

- X-ray powder diffraction (XRD)
- Transmission Electron Microscopy (TEM)
- Vibrating Sample Magnetometer (VSM)
- Mössbauer Effect Spectroscopy
- Neutron Diffraction

Introduction

Magnetism

- Magnetic moments originate from unpaired electrons which causes orbital and spin moment.

1	2	3	4	5	6	7	8	9	10	11	12	13	14	15	16	17	18
H (-2,5)	all values given for a temperature of 300 K																He (-1,1)
Li 24	Be -23											B -19	C -22	N (-6,3)	O 7,9	F	Ne (-4,0)
Na 8.1	Mg 5.7											Al 21	Si -3,4	P -23	S -12	Cl (-22)	Ar (-11)
K 5.7	Ca 21	Sc 264	Ti 181	V 383	Cr 267	Mn 828	Fe 2.16	Co 1.76	Ni 0.61	Cu -9.7	Zn -12	Ga -23	Ge -7,3	As -5,4	Se -18	Br -16	Kr (-16)
Rb 4,4	Sr 36	Y 122	Zr 109	Nb 236	Mo 119	Tc 373	Ru 66	Rh 170	Pd 783	Ag -25	Cd -19	In -8,2	Sn 2,4	Sb -67	Te -24	I -22	Xe (-24)
Cs 5.3	Ba 6.7	La 63	Hf 71	Ta 175	W 78	Re 96	Os 15	Ir 37	Pt 264	Au -34	Hg -28	Tl -36	Pb -16	Bi -153	Po	At	Rn

diamagnetic

paramagnetic

ferromagnetic

Introduction

Magnetism

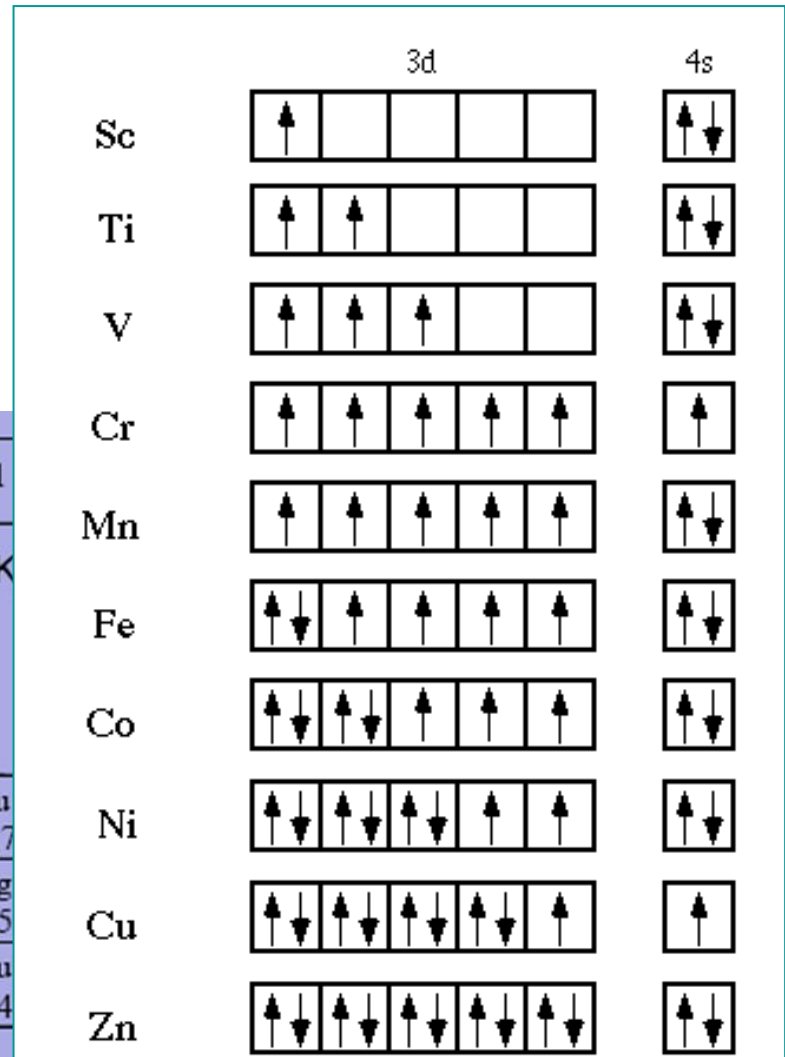
- Magnetic moments originate from unpaired electrons which causes orbital and spin moment.

1	2	3	4	5	6	7	8	9	10	11
H (-2,5)	all values given for a temperature of 300 K									
Li 24	Be -23									
Na 8.1	Mg 5.7									
K 5.7	Ca 21	Sc 264	Ti 181	V 383	Cr 267	Mn 828	Fe 2.16	Co 1.76	Ni 0.61	Cu -9.7
Rb 4,4	Sr 36	Y 122	Zr 109	Nb 236	Mo 119	Tc 373	Ru 66	Rh 170	Pd 783	Ag -25
Cs 5.3	Ba 6.7	La 63	Hf 71	Ta 175	W 78	Re 96	Os 15	Ir 37	Pt 264	Au -34

diamagnetic

paramagnetic

ferromagnetic



Introduction

Magnetism

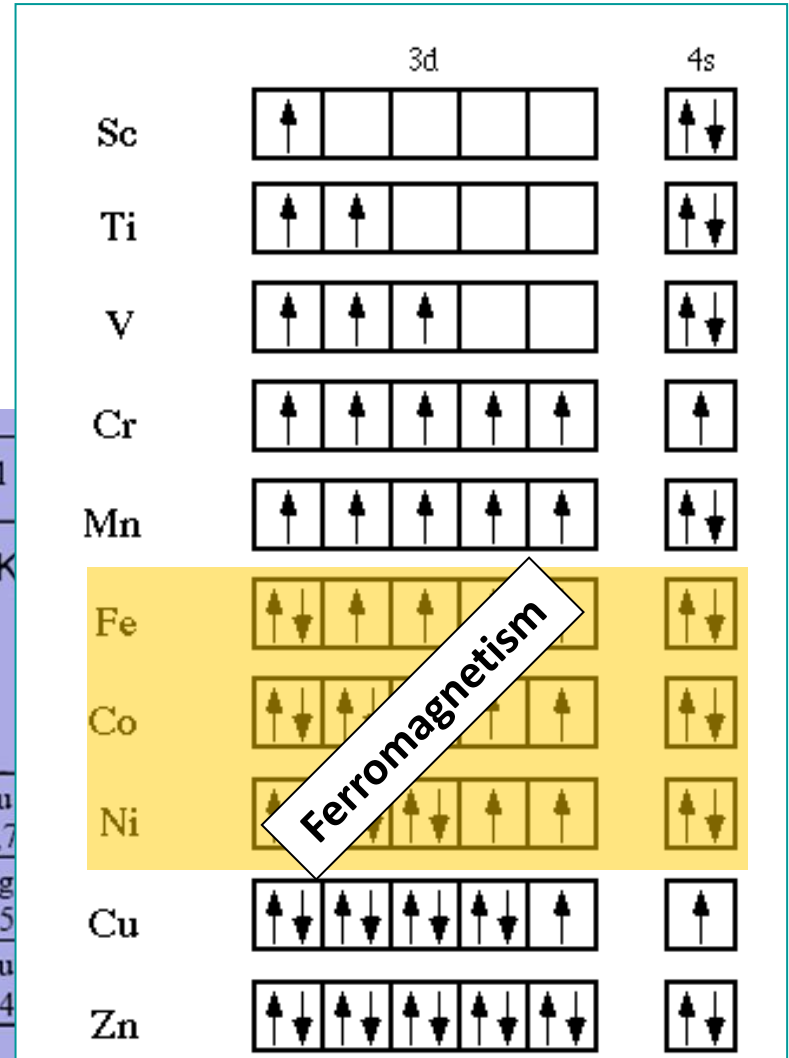
- Magnetic moments originate from unpaired electrons which causes orbital and spin moment.

1	2	3	4	5	6	7	8	9	10	11
H (-2,5)	all values given for a temperature of 300 K									
Li 24	Be -23									
Na 8.1	Mg 5.7									
K 5.7	Ca 21	Sc 264	Ti 181	V 383	Cr 267	Mn 828	Fe 2.16	Co 1.76	Ni 0.61	Cu -9.7
Rb 4,4	Sr 36	Y 122	Zr 109	Nb 236	Mo 119	Tc 373	Ru 66	Rh 170	Pd 783	Ag -25
Cs 5.3	Ba 6.7	La 63	Hf 71	Ta 175	W 78	Re 96	Os 15	Ir 37	Pt 264	Au -34

diamagnetic

paramagnetic

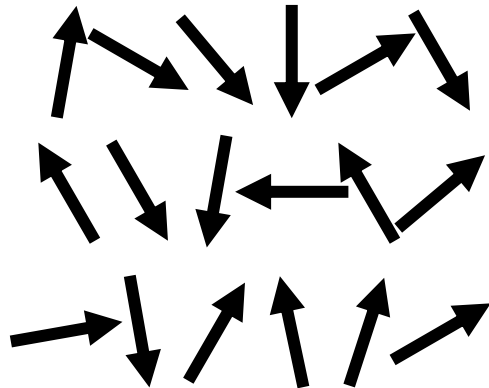
ferromagnetic



Exchange interaction **vs** thermal fluctuation

Heisenberg Hamiltonian

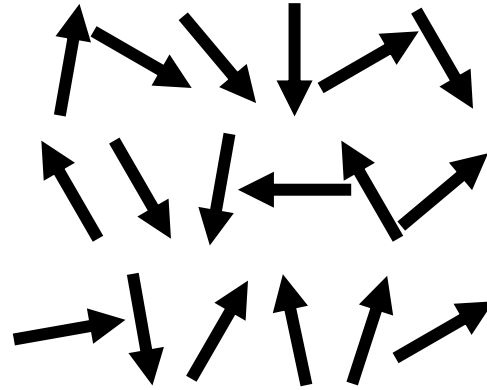
$$H = J \sum_{\langle ij \rangle} \vec{S}_i \cdot \vec{S}_j$$



Randomizing thermal effects

$$k_B T$$

Paramagnetthermal fluctuation higher
than the exchange energy

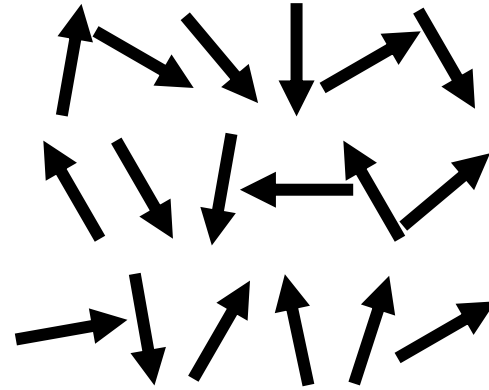


Paramagnet

Thermal fluctuation stronger
than the exchange energy

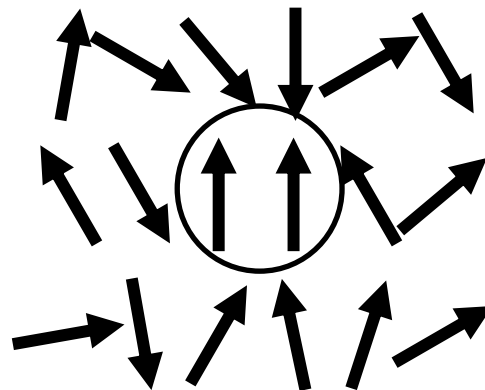
Paramagnet

Thermal fluctuation stronger than the exchange energy



Lowering T

Thermal fluctuation weaker than the exchange energy



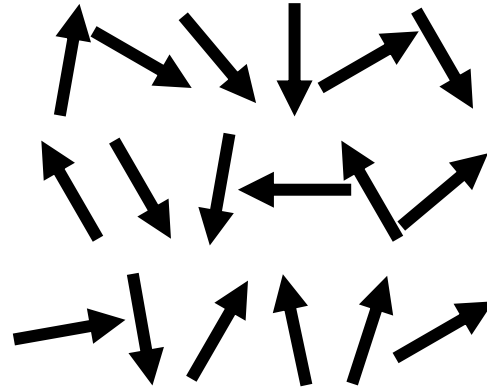
Ferromagnetic

J -ve

Growing magnetic correlation length
From **short range** to **long range**

Paramagnet

Thermal fluctuation stronger than the exchange energy



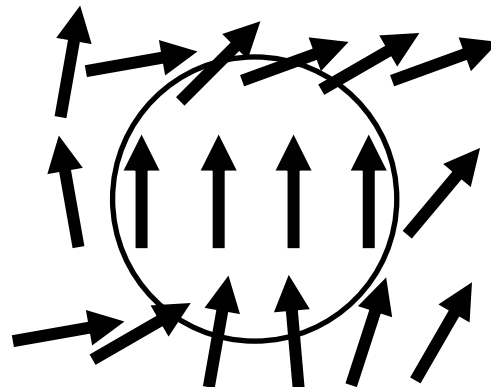
Lowering T

Thermal fluctuation weaker than the exchange energy



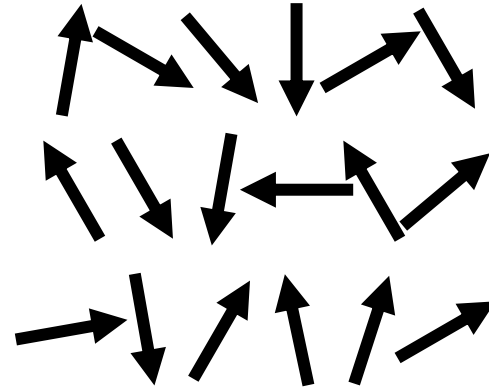
Growing magnetic correlation length

From **short range** to **long range**



Ferromagnetic

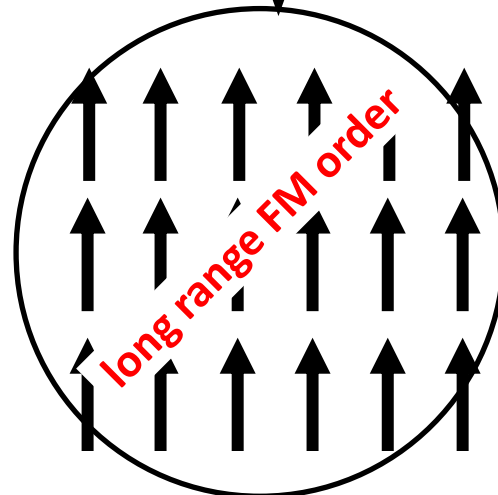
J -ve



Paramagnet

Thermal fluctuation stronger than the exchange energy

T below T_c

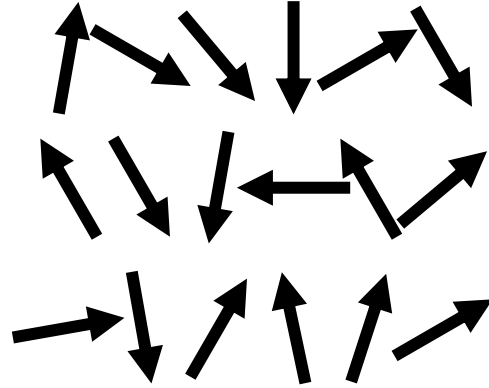


Thermal fluctuation weaker than the exchange energy

Growing magnetic correlation length
From **short range** to **long range**

Ferromagnetic

J -ve



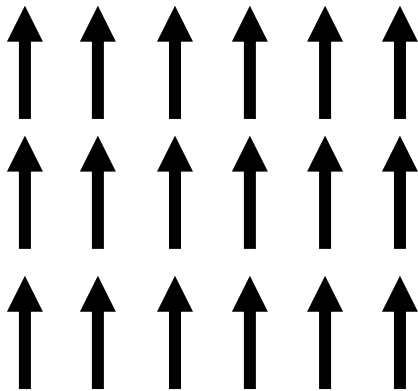
Paramagnet

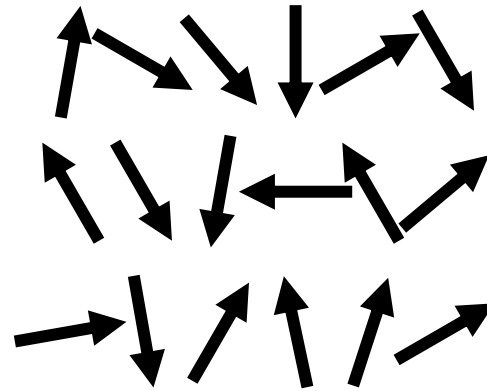
Thermal fluctuation stronger than the exchange energy

Lowering T below T_C or T_N



Thermal fluctuation weaker than the exchange energy





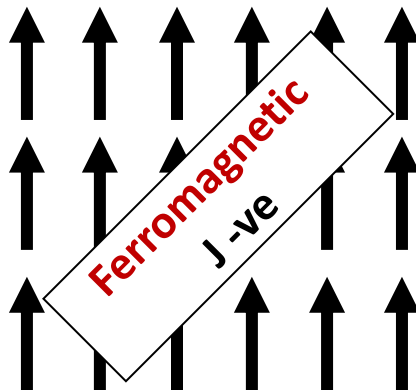
Paramagnet

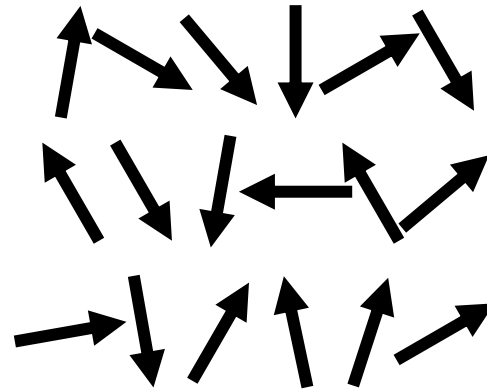
Thermal fluctuation stronger than the exchange energy

Lowering T below T_C or T_N



Thermal fluctuation weaker than the exchange energy





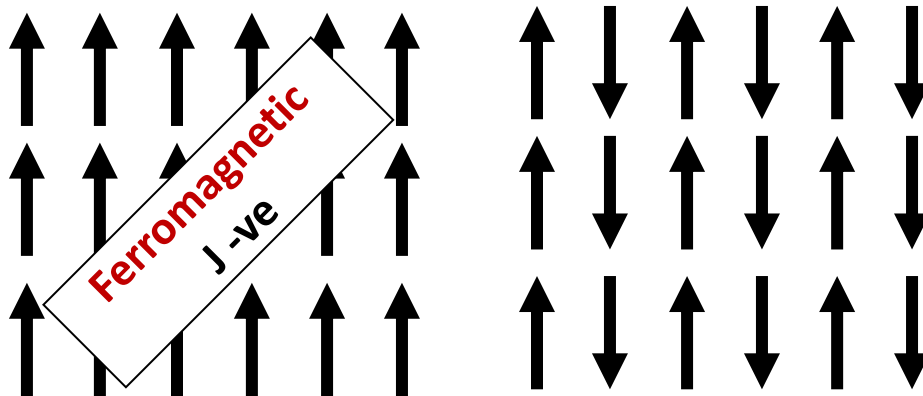
Paramagnet

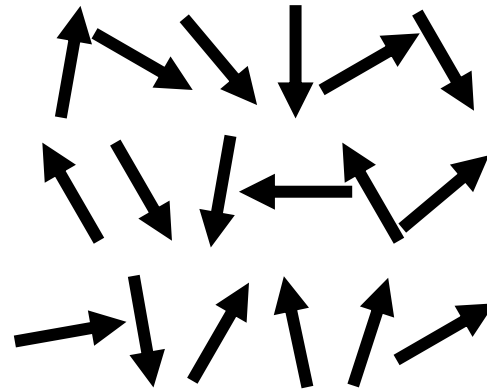
Thermal fluctuation stronger than the exchange energy

Lowering T below T_C or T_N



Thermal fluctuation weaker than the exchange energy



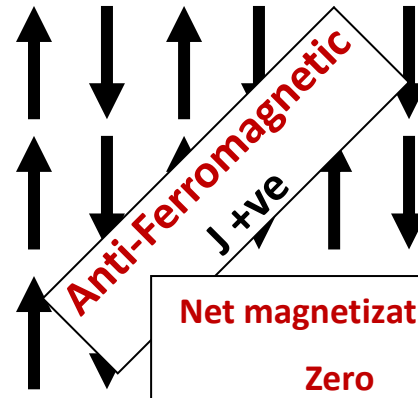
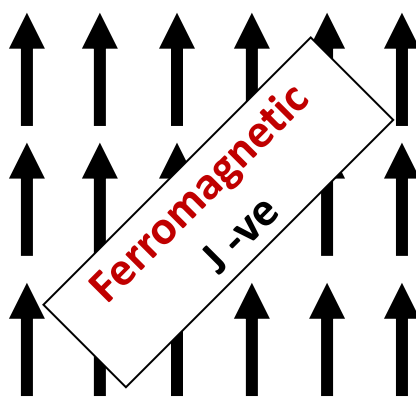


Paramagnet

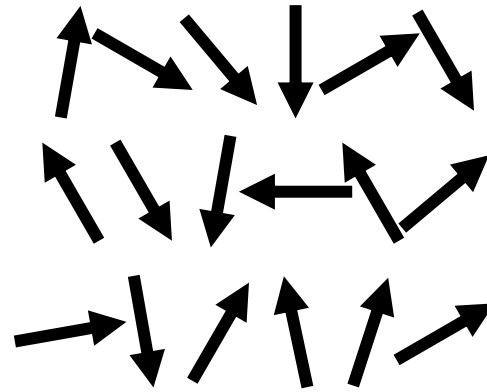
Thermal fluctuation stronger than the exchange energy

Lowering T below T_C or T_N

Thermal fluctuation weaker than the exchange energy



Net magnetization =
Zero

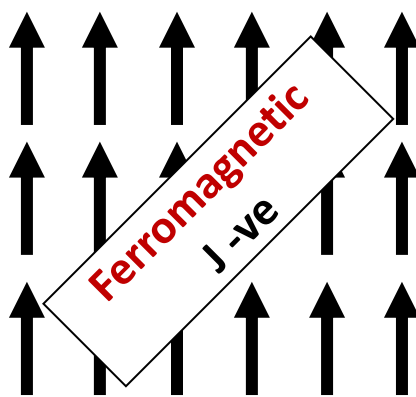


Paramagnet

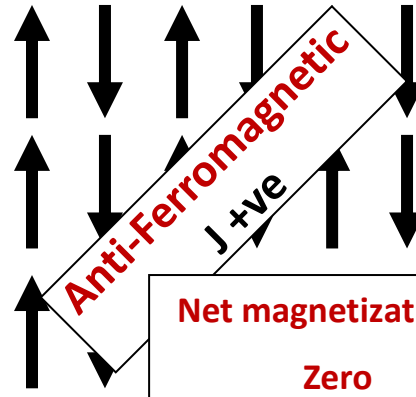
Thermal fluctuation stronger than the exchange energy

Lowering T below T_C or T_N

Thermal fluctuation weaker than the exchange energy

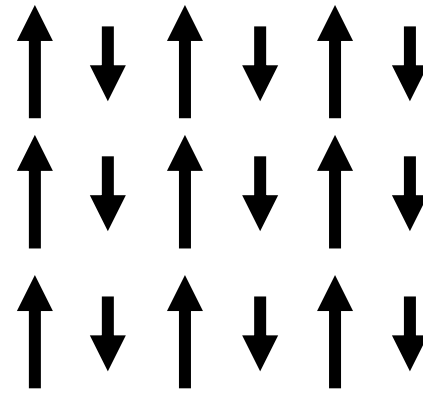


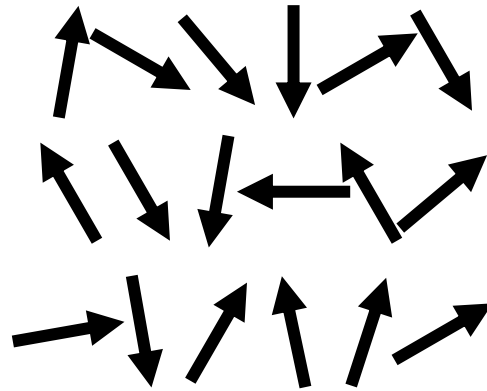
Ferromagnetic
 J -ve



Anti-Ferromagnetic
 J +ve

Net magnetization =
Zero



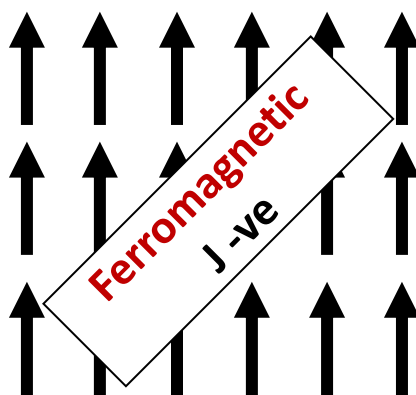


Paramagnet

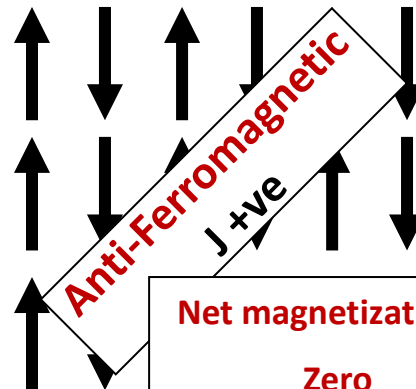
Thermal fluctuation stronger than the exchange energy

Lowering T below T_C or T_N

Thermal fluctuation weaker than the exchange energy

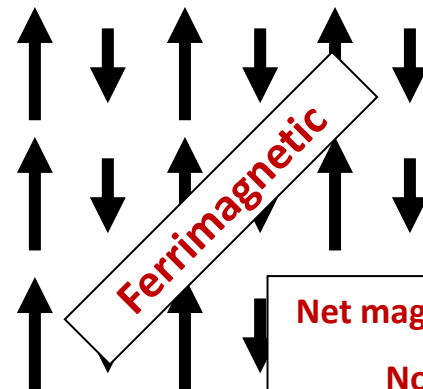


Ferromagnetic
 J -ve



Anti-Ferromagnetic
 J +ve

Net magnetization =
Zero



Ferrimagnetic

Net magnetization =
Non Zero

Introduction

Magnetism

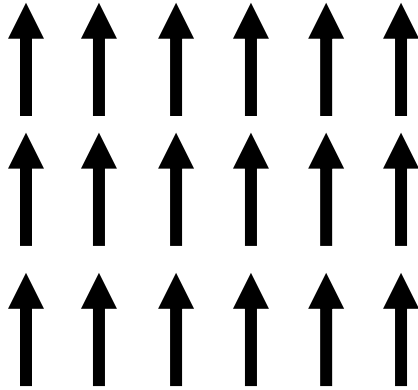
Landau theory for phase transition

Order Parameter

Landau theory for phase transition

Order Parameter

Ferromagnetic



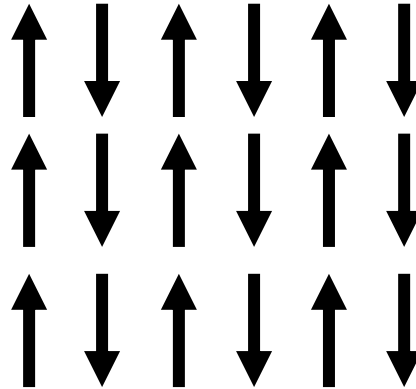
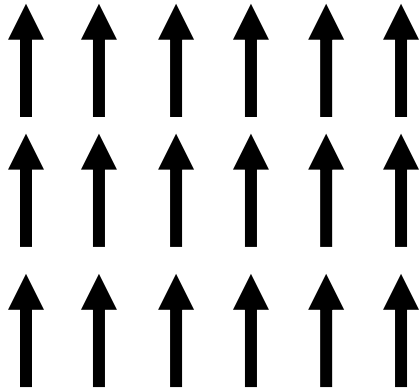
Internal field

Landau theory for phase transition

Order Parameter

Ferromagnetic

Anti-Ferromagnetic

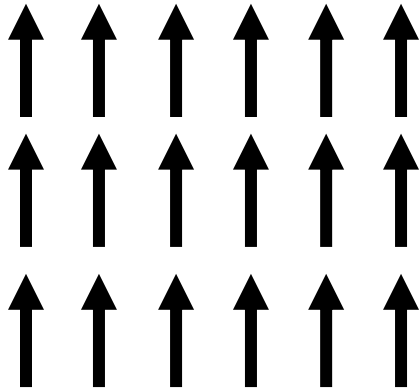


Internal field

Landau theory for phase transition

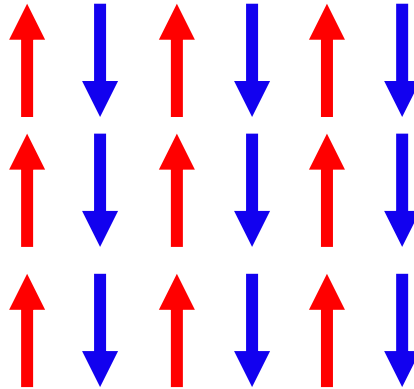
Order Parameter

Ferromagnetic



Internal field

Anti-Ferromagnetic

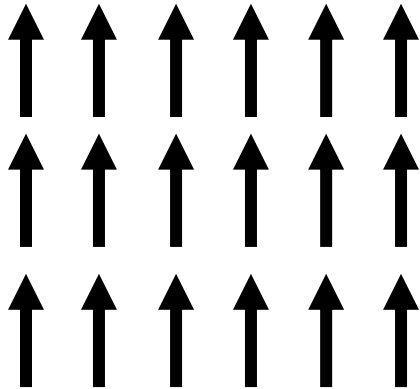


Sub lattice magnetization

Landau theory for phase transition

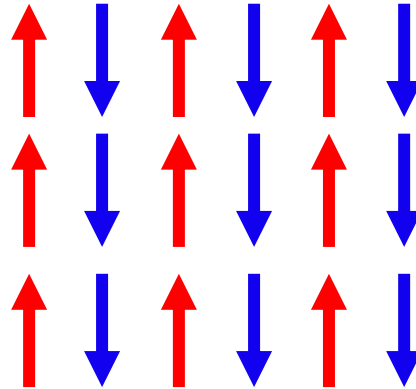
Order Parameter

Ferromagnetic



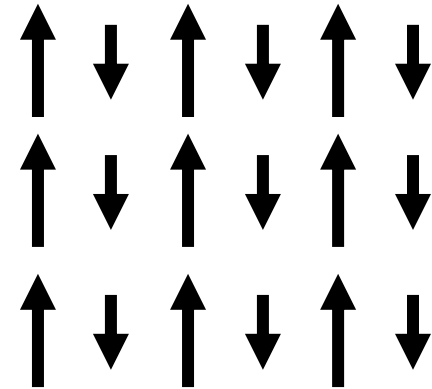
Internal field

Anti-Ferromagnetic

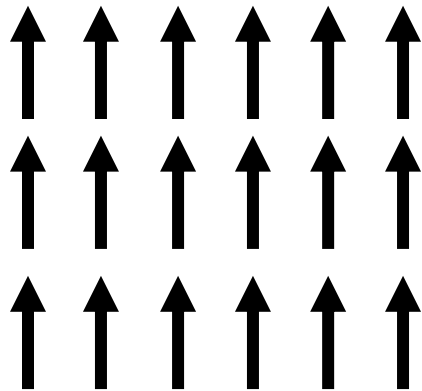


Sub lattice magnetization

Ferrimagnetic



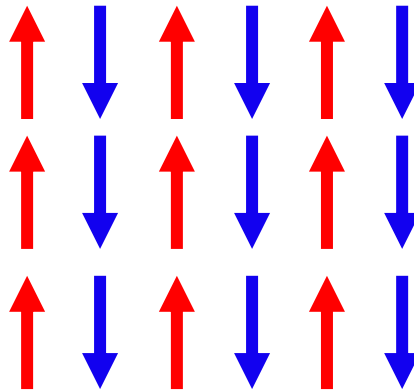
Ferromagnetic



Internal field

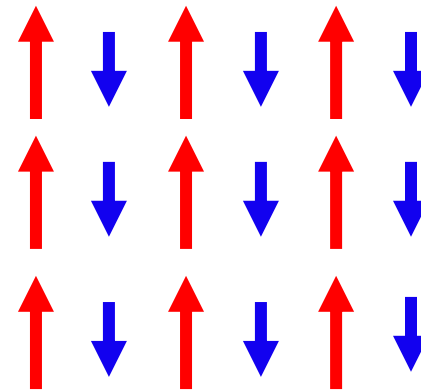
Order Parameter

Anti-Ferromagnetic



Sub lattice magnetization

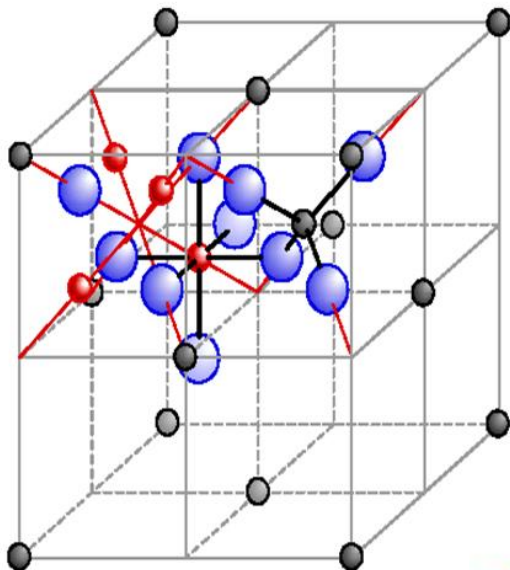
Ferrimagnetic



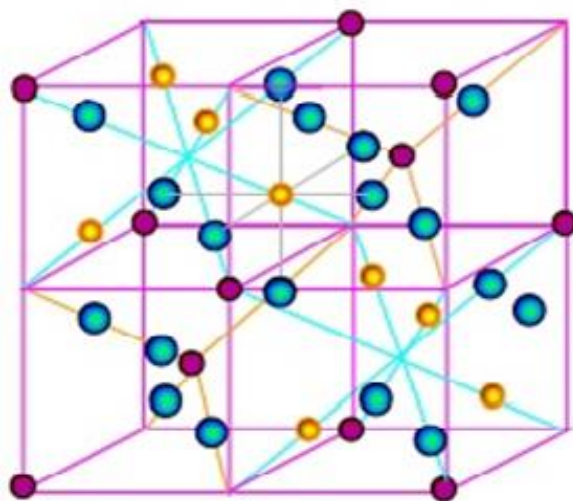
Sub lattice magnetization

Spinel Ferrite

Introduction



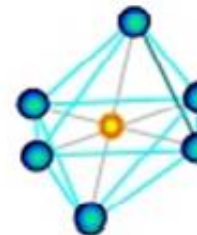
Spinel structure MB_2O_4



● (A)- site ions
● [B]- site ions
● Oxygen ions

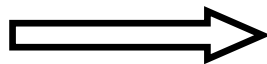


Tetrahedral (A) site



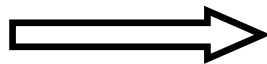
Octahedral [B] site

64 tetrahedral sites



8 occupied

32 octahedral sites



16 occupied

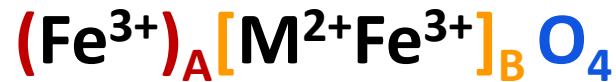
Regular spinel structure

Divalent metal ions in the tetrahedral (A)-site and trivalent metal ions in the octahedral [B]-site



Inverse spinel structure

Half of the [B]-sites (8 sites) are occupied by divalent metal ions and the remaining half of the [B]-sites (8 sites) and all the (A)-sites are occupied by the trivalent metal ions



Partial inverse spinel structure



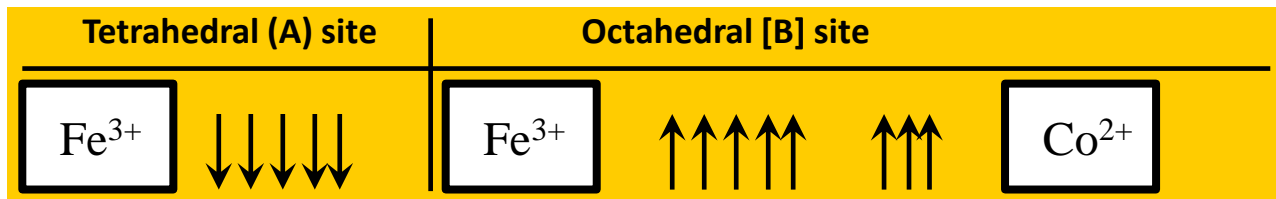
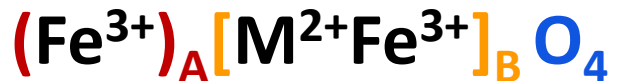
δ degree of inversion

Spinel Ferrite

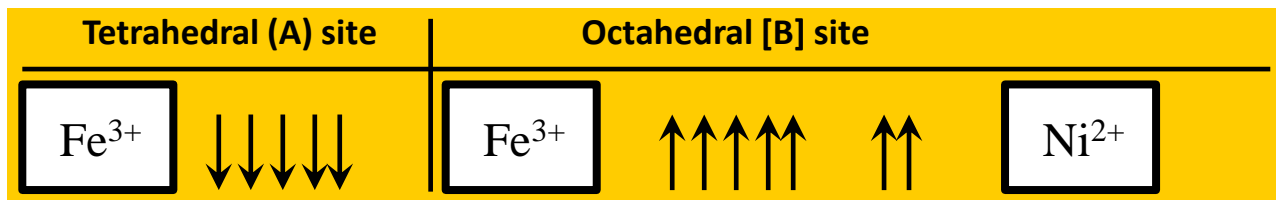
Introduction

Néel theory:

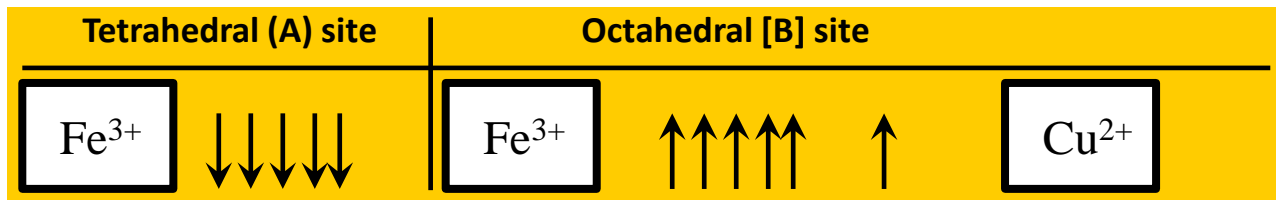
$$M = M_B - M_A$$



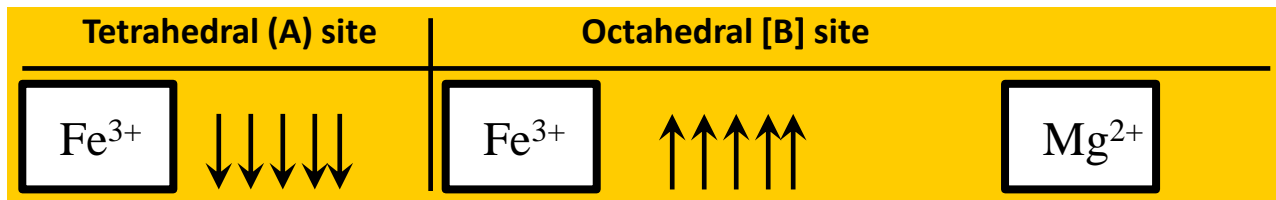
$$3\mu_B$$



$$2\mu_B$$



$$1\mu_B$$



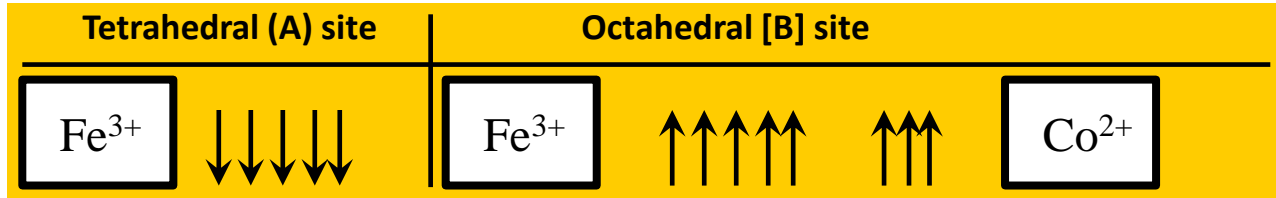
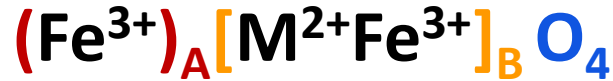
$$0\mu_B$$

Spinel Ferrite

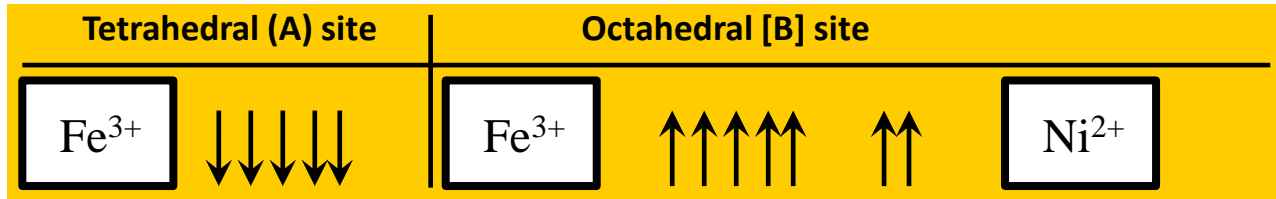
Introduction

Néel theory:

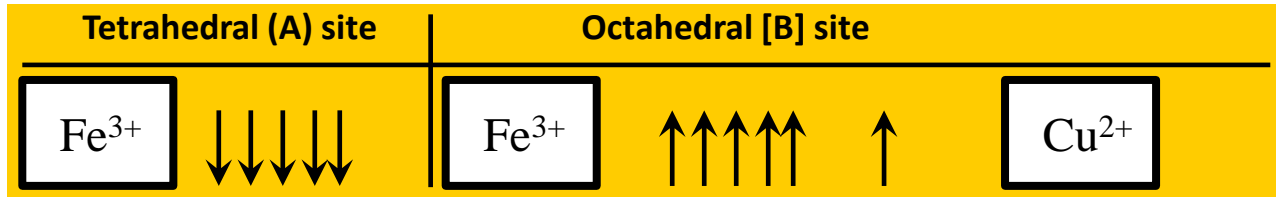
$$M = M_B - M_A$$



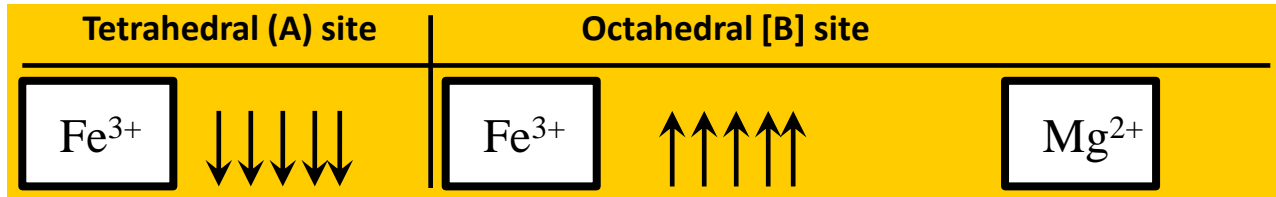
$$3\mu_B$$



$$2\mu_B$$



$$1\mu_B$$



$$0\mu_B$$

- 1- Complex exchange interactions of the different cations between and within the A & B sites.
- 2- Effect of the reduced particle size.
- 3- Effect of defects and lattice deformation.

Applications of Ferrites

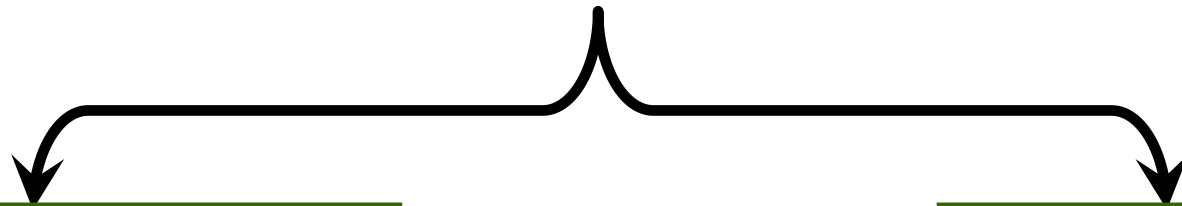
➤ Ferrites have very wide rang of applications:

- ❖ In radio receivers to increase the sensitivity and selectivity of the receiver.
- ❖ As cores in audio and TV transformer
- ❖ In digital computers and data processing circuits.
- ❖ To produce low frequency ultra sonic waves by magnetostriction principle.
- ❖ In high-power microwave Components and Industrial Microwave Systems..
- ❖ In the design of ferromagnetic amplifiers of microwave signals.
- ❖ In instruments like galvanometers, ammeter, voltmeter, flex meters, speedometers, wattmeter, compasses and recorders
- ❖ In high power circulators, isolators, couplers, phase shifters, filters, and loads for industrial, radar, medical and high energy physics applications.

Tunning Ferrite Properties

Controlling particle size

R&TM-doping



Spinel Ferrite

Introduction

Ion	A-site (Å)	B-site (Å)
$r(\text{Sm}^{3+})$	-	0.958
$r(\text{Gd}^{3+})$	-	0.938
$r(\text{Ce}^{3+})$	-	1.14

VS

Ion	A-site (Å)	B-site (Å)
$r(\text{Fe}^{3+})$	0.49	0.645
$r(\text{Ni}^{2+})$	0.55	0.69
$r(\text{Co}^{2+})$	0.38	0.745

R^{3+} ions doping

B-site

Lattice distortion

Diffuse to the grain boundaries

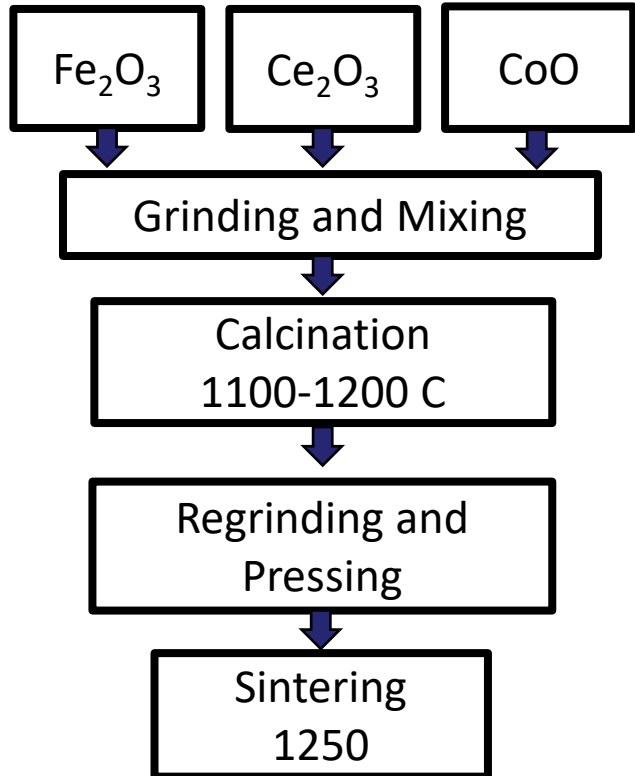
Extra amorphous or crystalline phases

Decrease the particle size

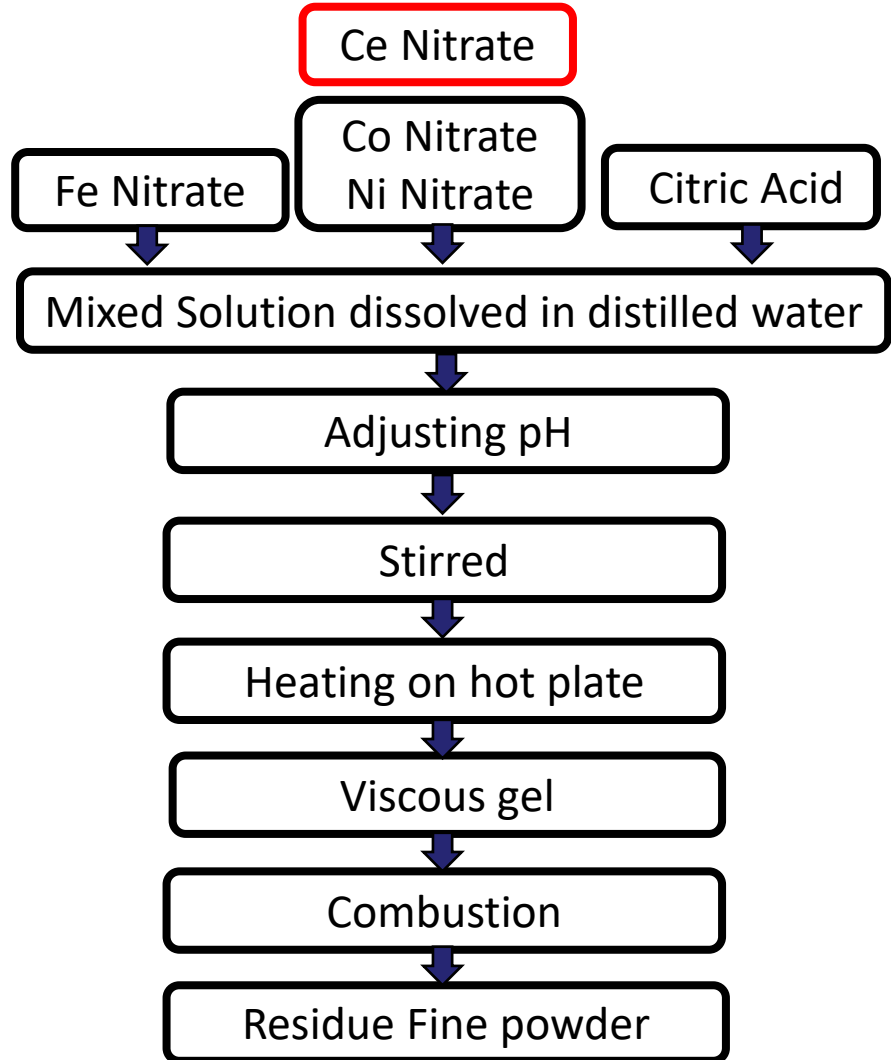
Experimental

Preparation

Standard Ceramic Method



SOL-GEL Method



Preparation Methods

Solid State Reaction

Transition metal-Rareearth Oxides

Expensive

High Temperatures

Energy consuming

Bulk Material

Particle size - No control

Sol-gel

Transition metal-Rareearth Nitrates

Reduced Cost

Low Temperatures

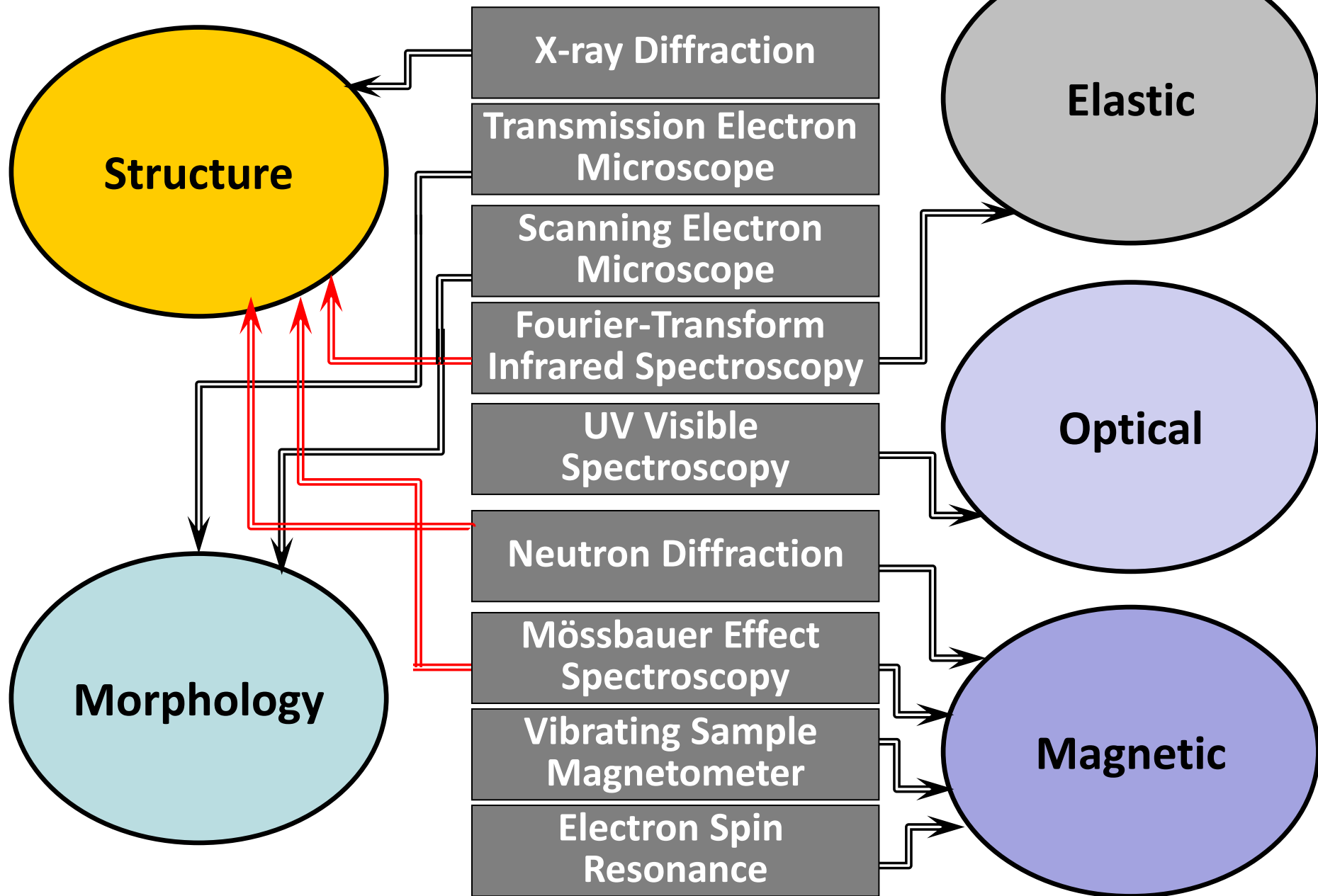
Energy saving

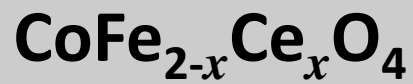
Nano Material

Controlled Particle size

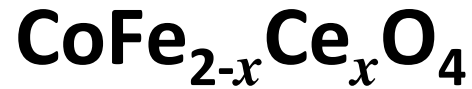
Experimental

Techniques





In this presentation



$x=0, 0.01, 0.03, 0.05, 0.07$ and 0.1

Sol-gel

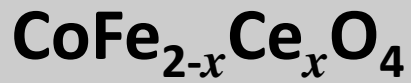
Transmission Electron
Microscope

X-ray Diffraction

Vibrating Sample
Magnetometer

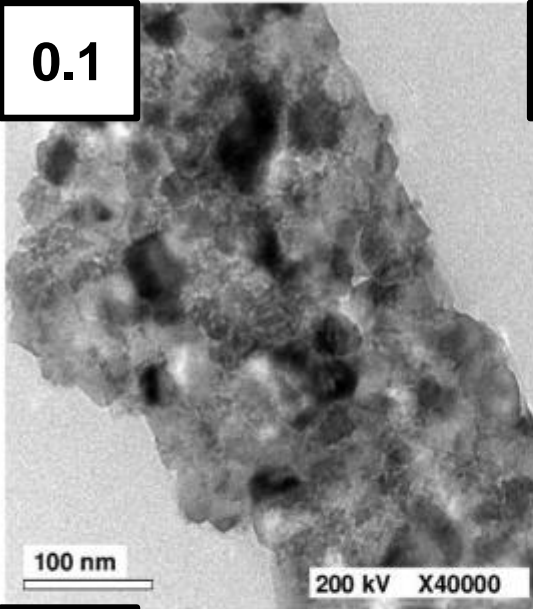
Neutron Diffraction

Mössbauer Effect
Spectroscopy

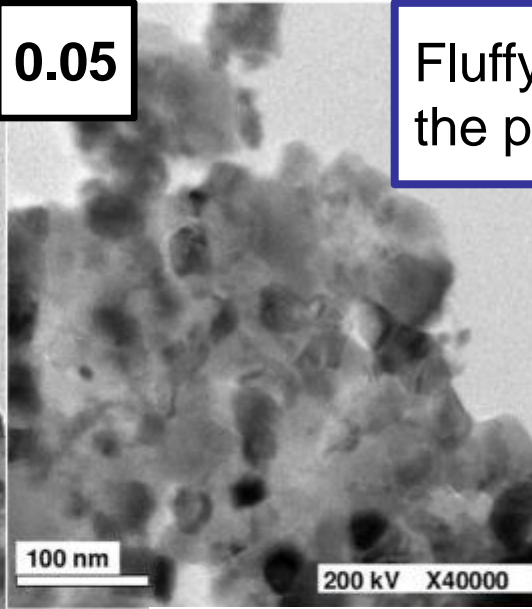


TEM

0.1

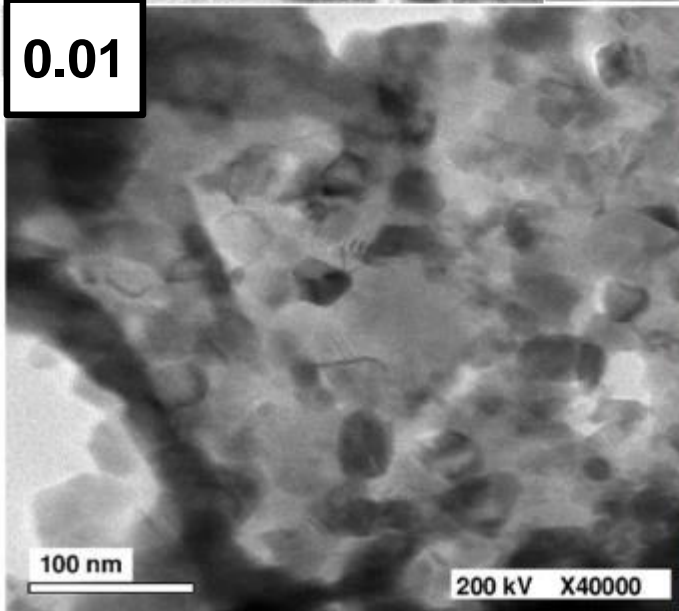


0.05



Fluffy final product for the prepared samples.

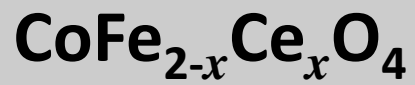
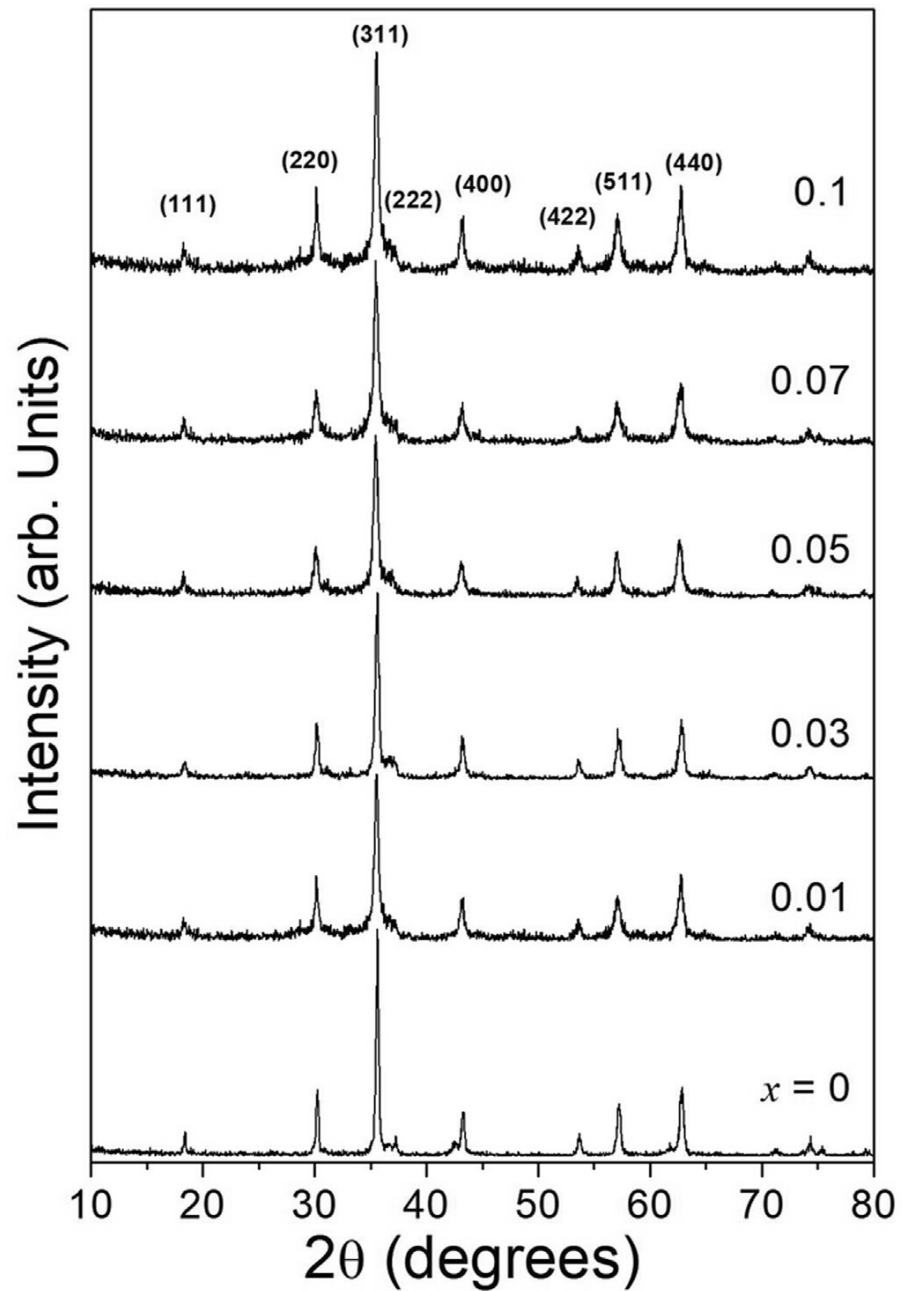
0.01

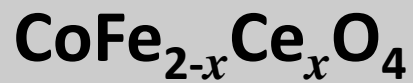
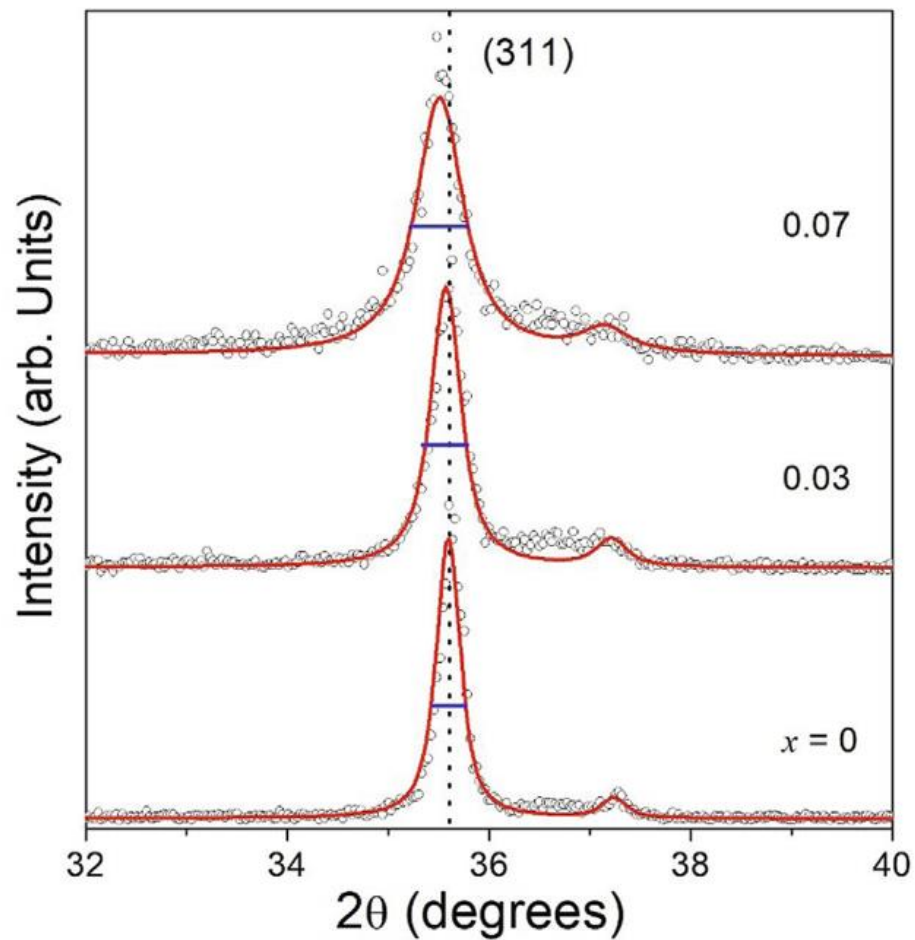
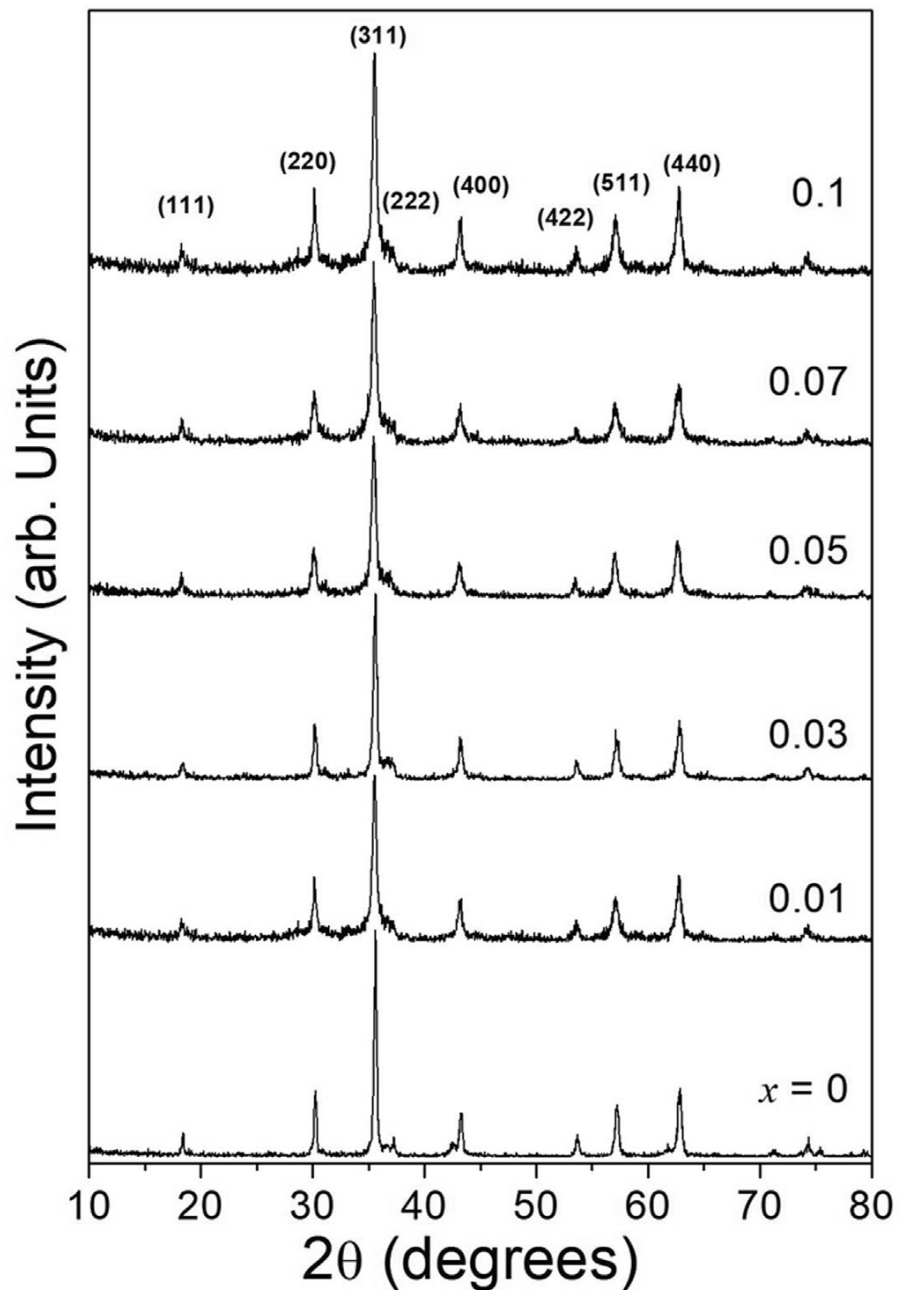


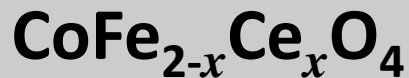
HR-TEM Micrographs

- Nano size
- Spherical shape

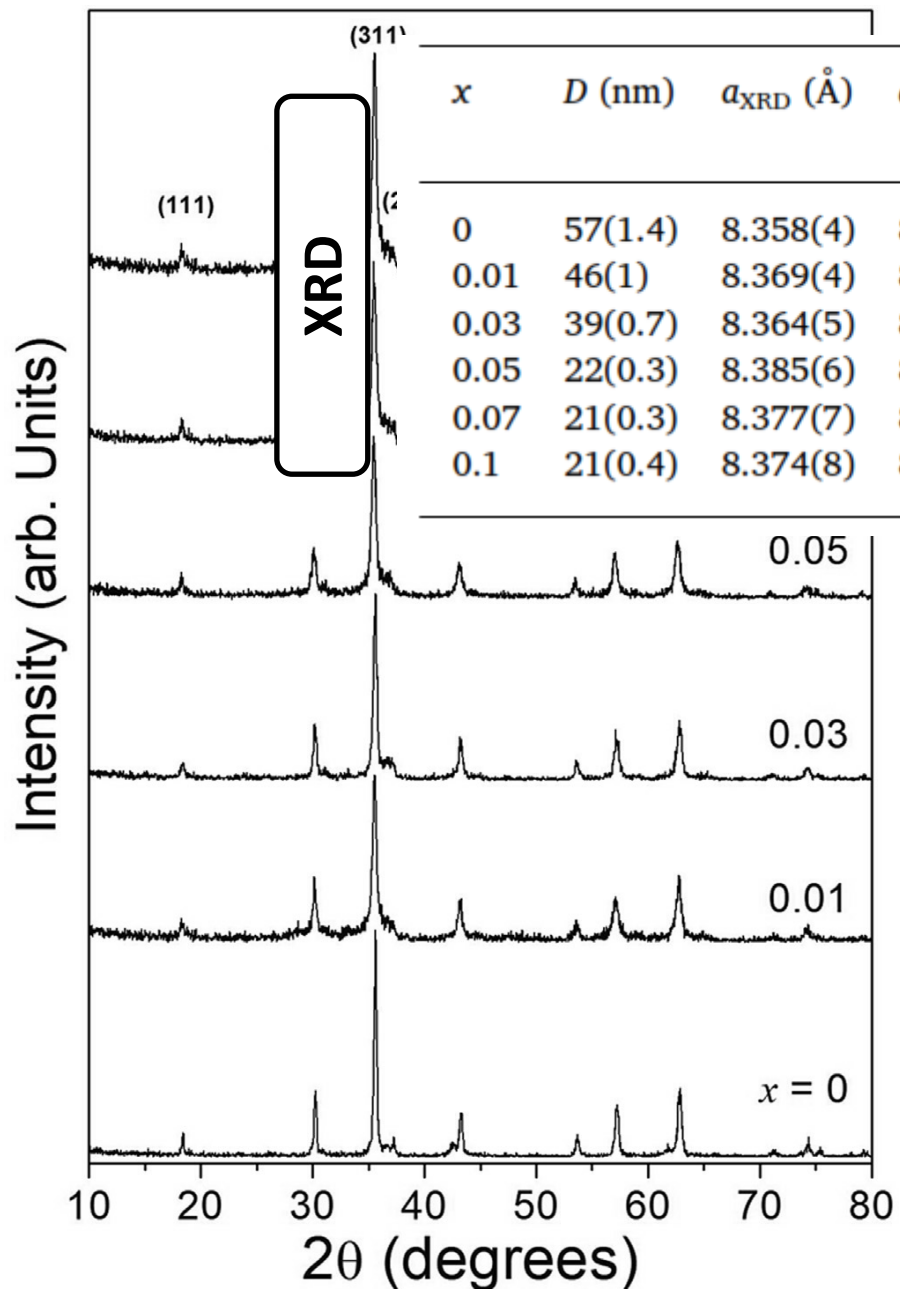


**XRD**

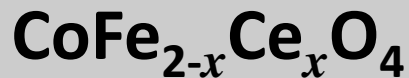
**XRD**



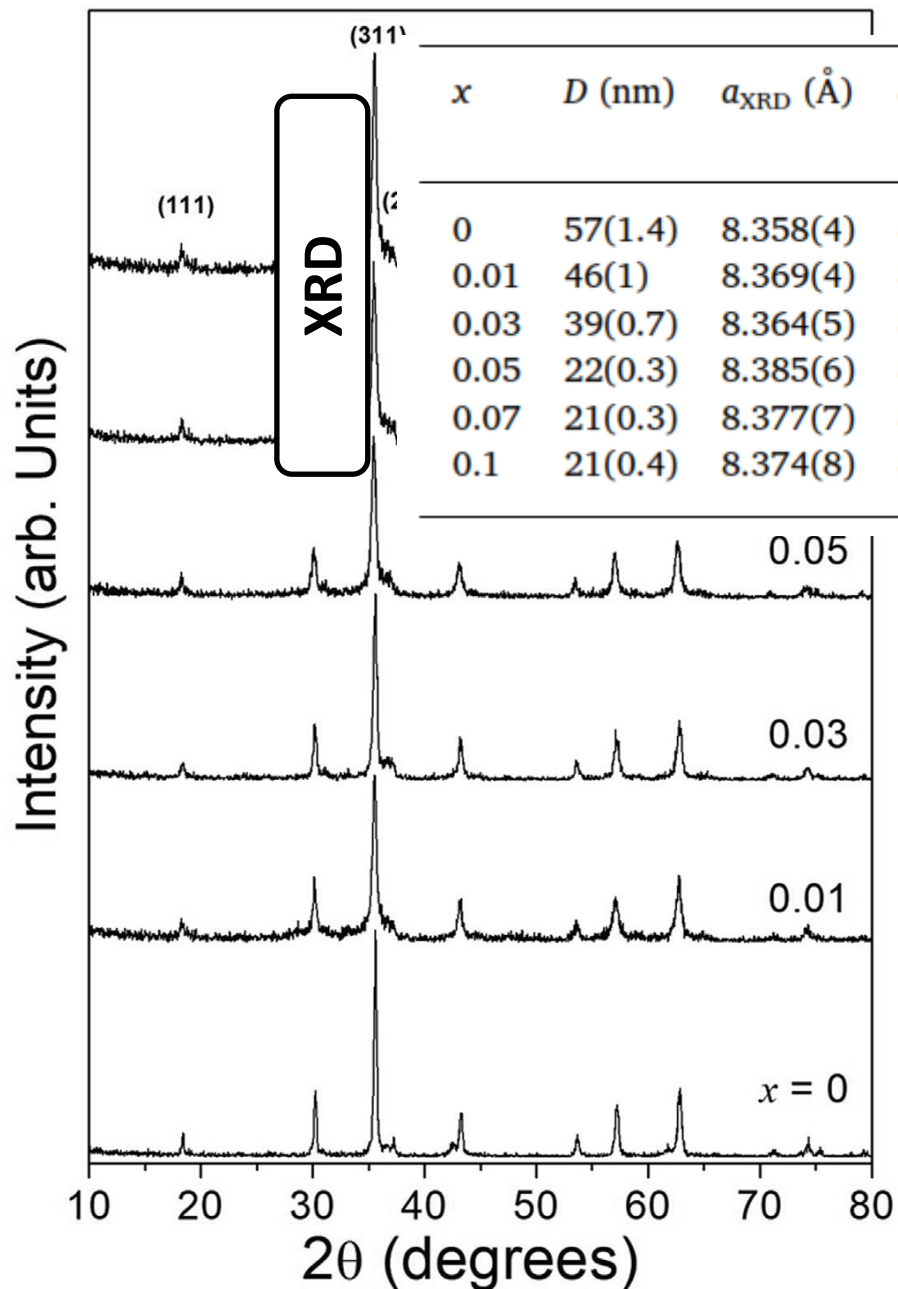
XRD



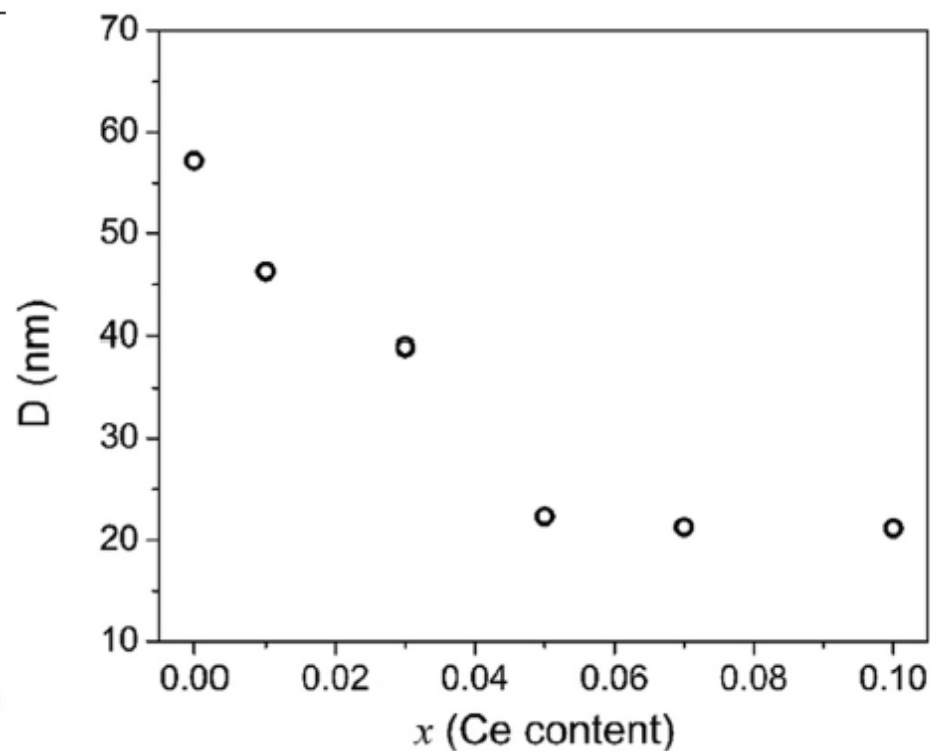
x	D (nm)	a_{XRD} (Å)	a_{th} (Å)	A-O cal. (Å)	B-O cal. (Å)	u^{3m} (Å)	u^{43m} (Å)
0	57(1.4)	8.358(4)	8.367	1.859	2.064	0.272	0.397
0.01	46(1)	8.369(4)	8.346	1.849	2.062	0.273	0.398
0.03	39(0.7)	8.364(5)	8.348	1.846	2.064	0.273	0.398
0.05	22(0.3)	8.385(6)	8.33	1.836	2.064	0.274	0.399
0.07	21(0.3)	8.377(7)	8.321	1.829	2.064	0.274	0.399
0.1	21(0.4)	8.374(8)	8.328	1.826	2.068	0.274	0.399

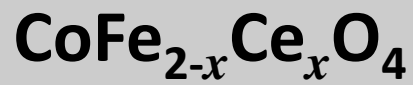


XRD

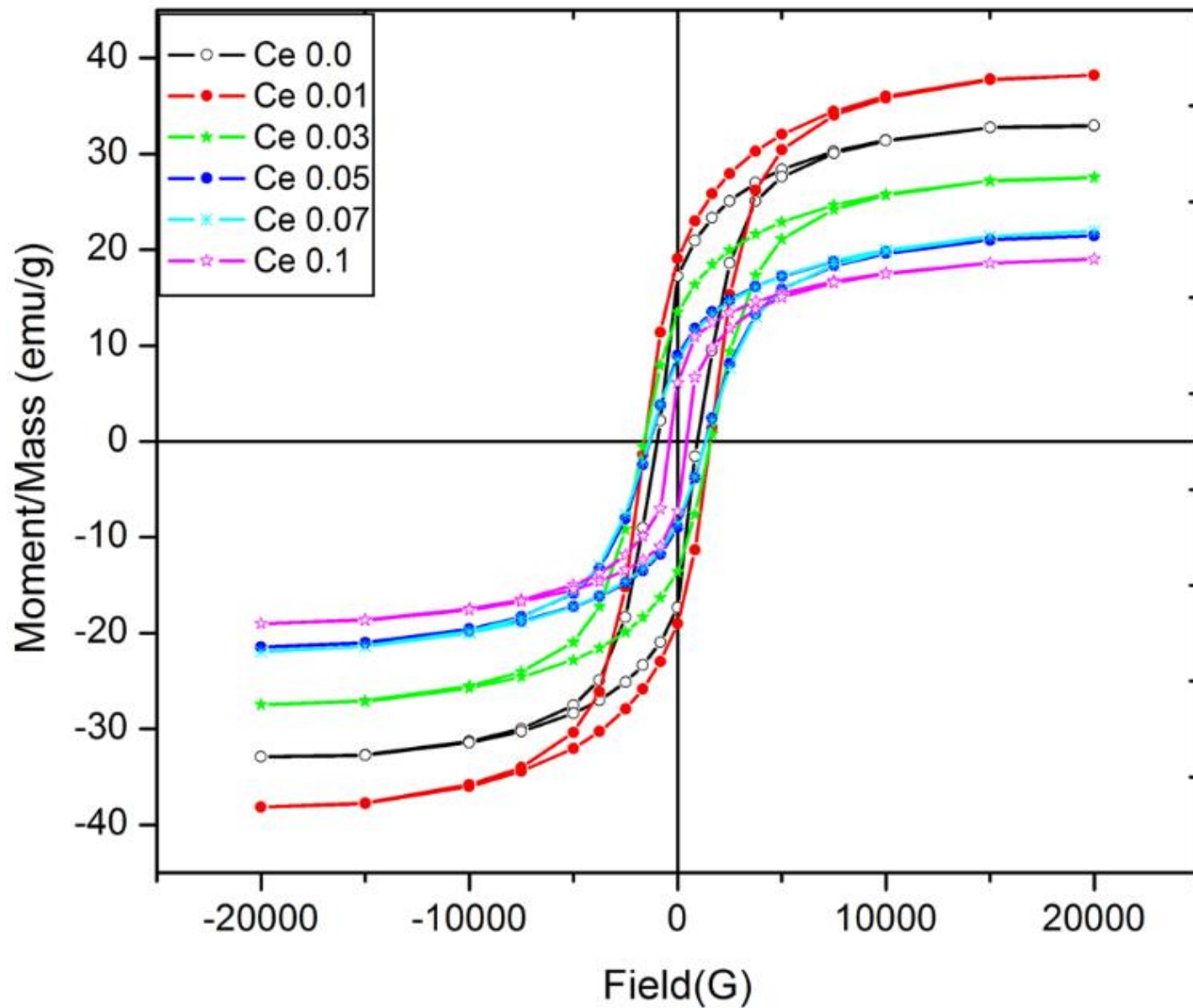


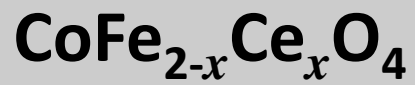
x	D (nm)	a_{XRD} (Å)	a_{th} (Å)	A-O cal. (Å)	B-O cal. (Å)	u^{3m} (Å)	u^{43m} (Å)
0	57(1.4)	8.358(4)	8.367	1.859	2.064	0.272	0.397
0.01	46(1)	8.369(4)	8.346	1.849	2.062	0.273	0.398
0.03	39(0.7)	8.364(5)	8.348	1.846	2.064	0.273	0.398
0.05	22(0.3)	8.385(6)	8.33	1.836	2.064	0.274	0.399
0.07	21(0.3)	8.377(7)	8.321	1.829	2.064	0.274	0.399
0.1	21(0.4)	8.374(8)	8.328	1.826	2.068	0.274	0.399



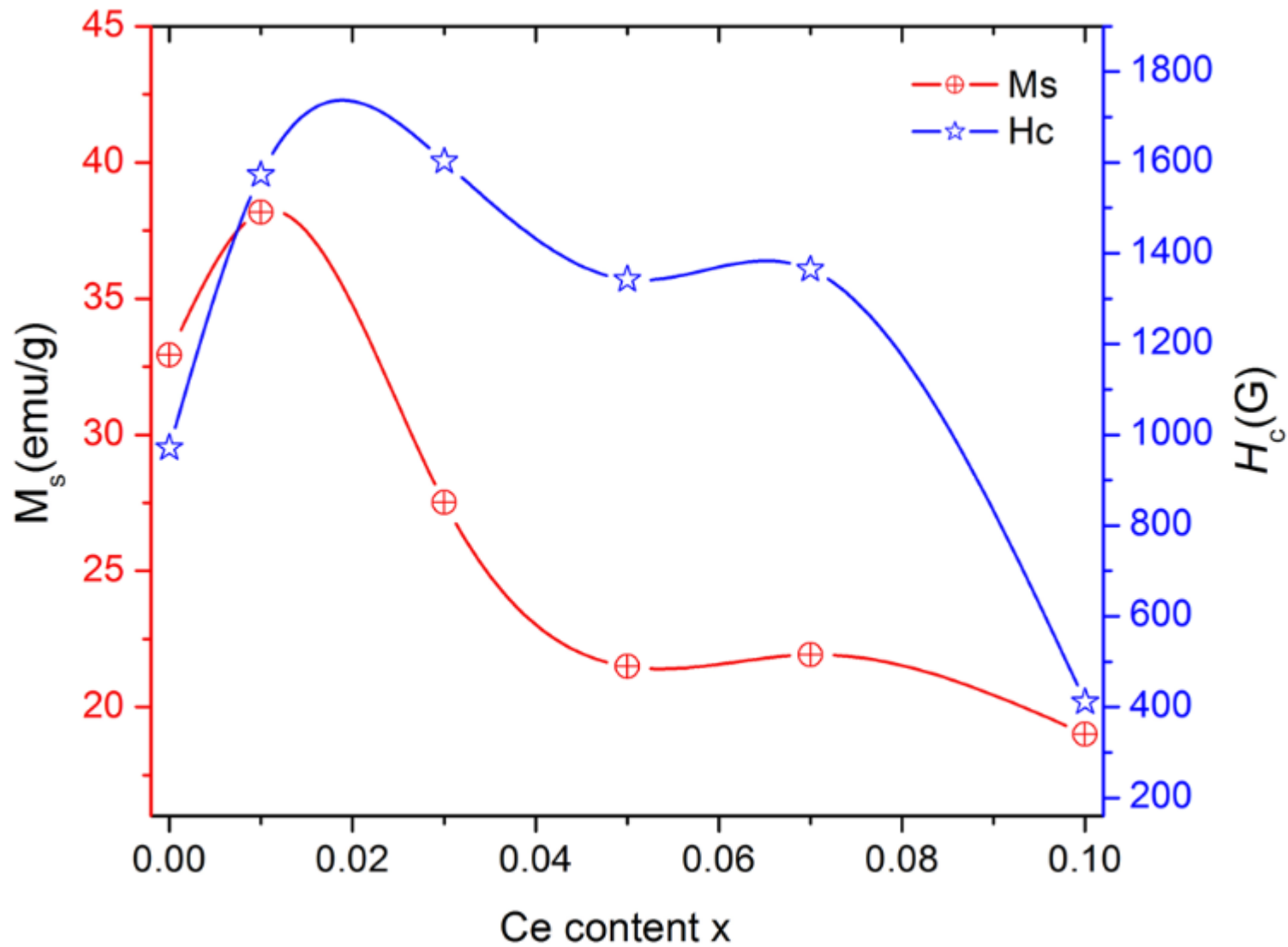


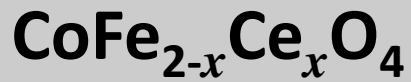
VSM





VSM

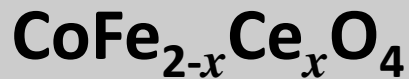




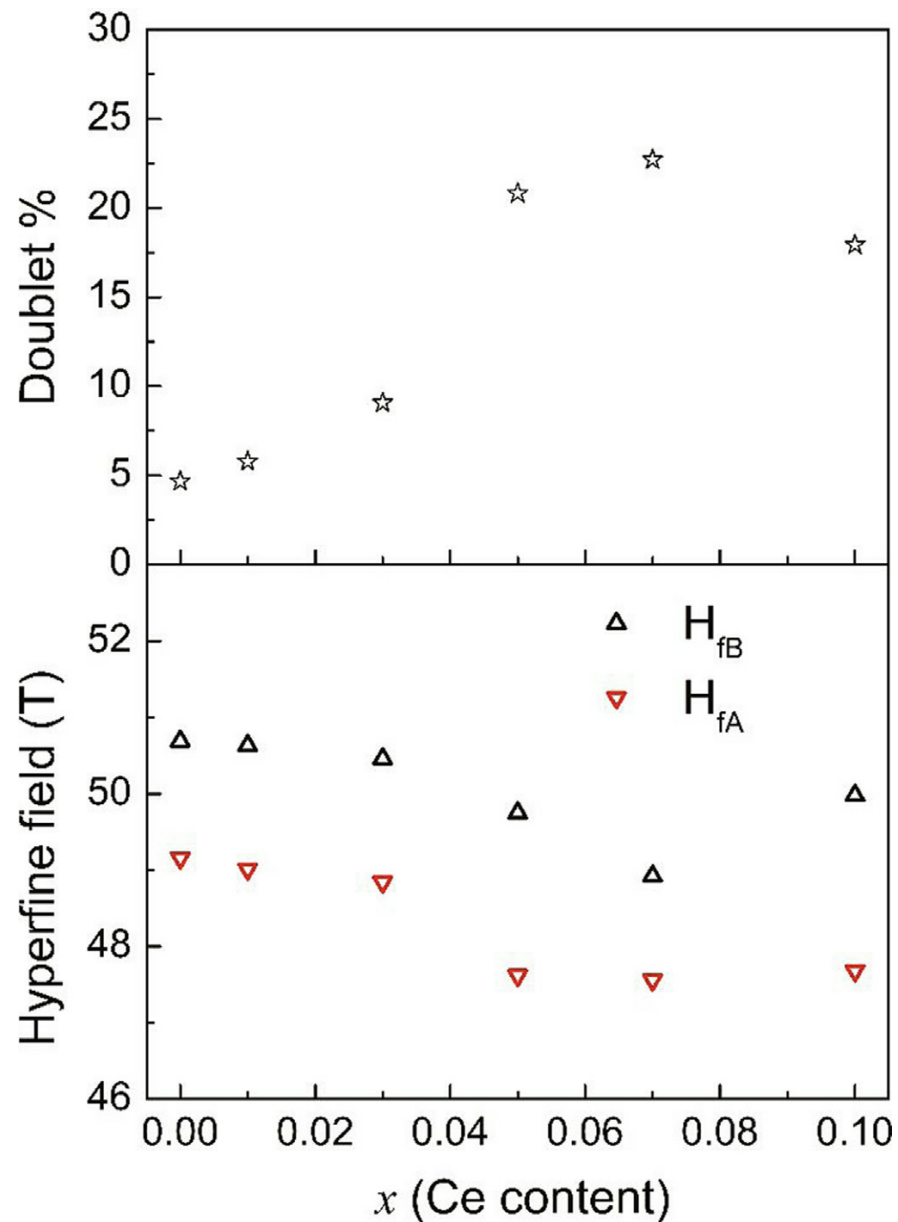
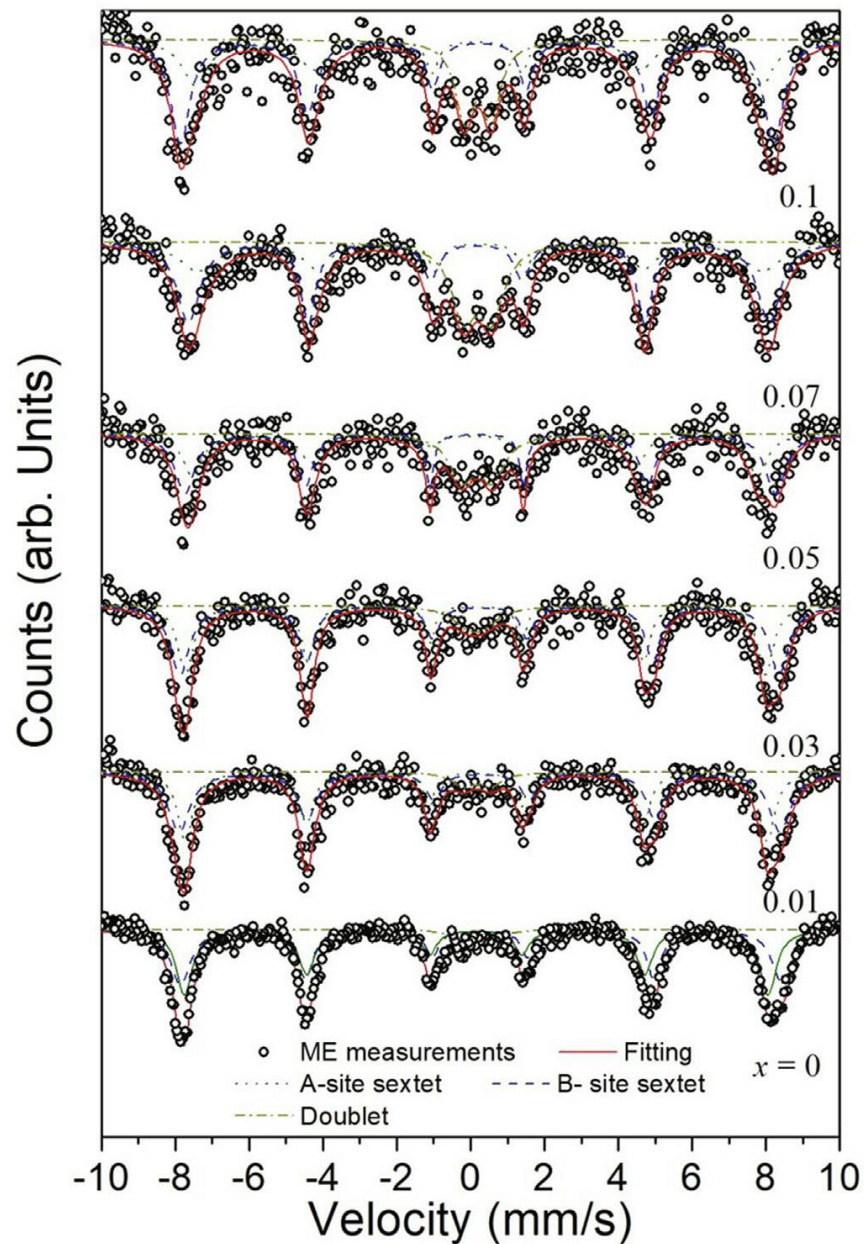
VSM

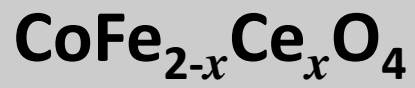
x	Saturation magnetization M_S (emu/g)	Coercivity H_c (G)	Remanent magnetization M_r (emu/g)	Magnetic moment n_B (μ_B)
0.0	32.9	972	17.3	1.38
0.01	38.2	1573	19.0	1.61
0.03	27.5	1603	13.6	1.17
0.05	21.5	1342	9.0	0.92
0.07	21.9	1364	8.6	0.94
0.1	19.0	411	6.7	0.83

Decreasing D \Longrightarrow Ms & Hc

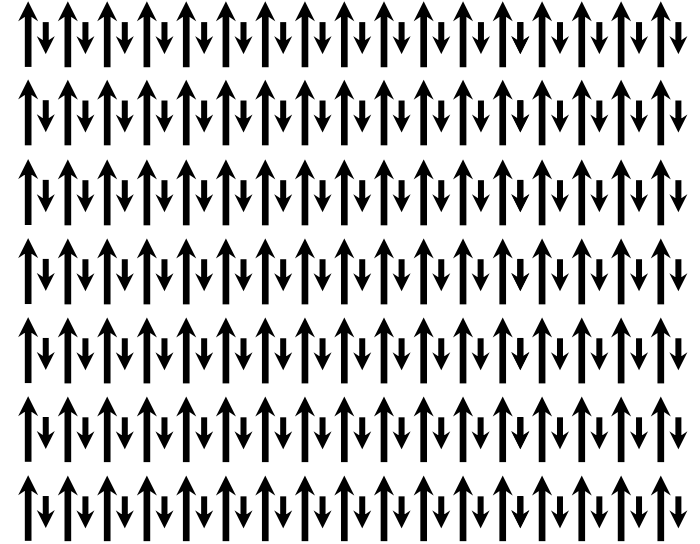


ME

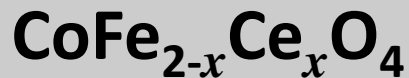




ME

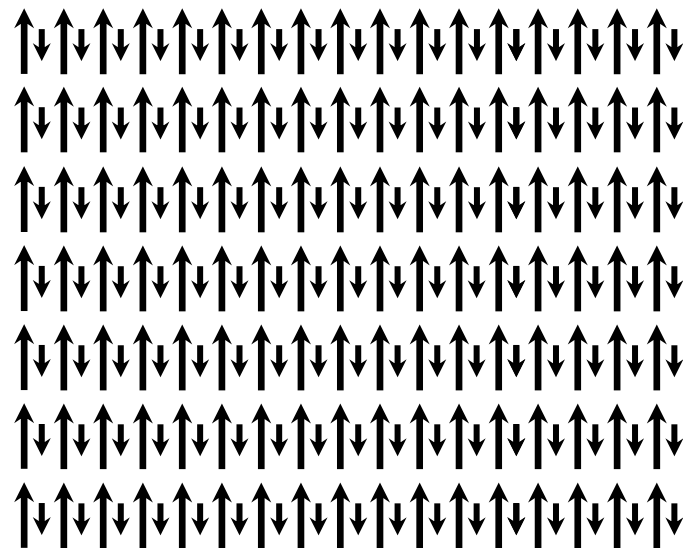
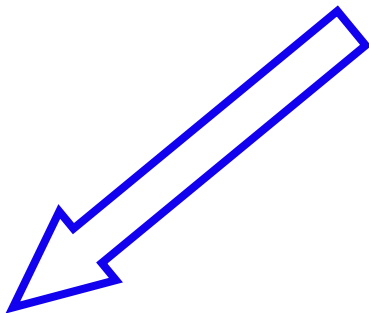
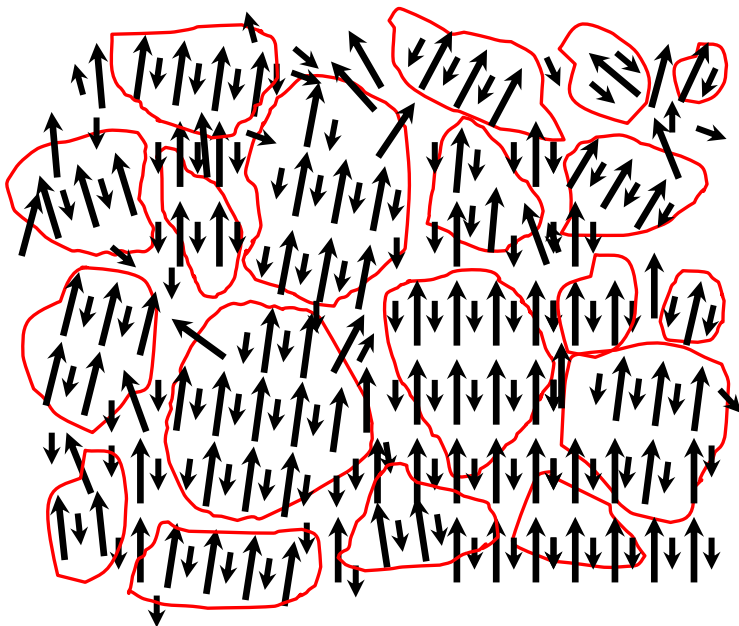


Typical long range ferrimagnetic order



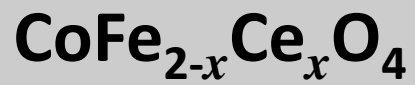
ME

Nano Scale: Small grain sizes (D)
with short range magnetic order

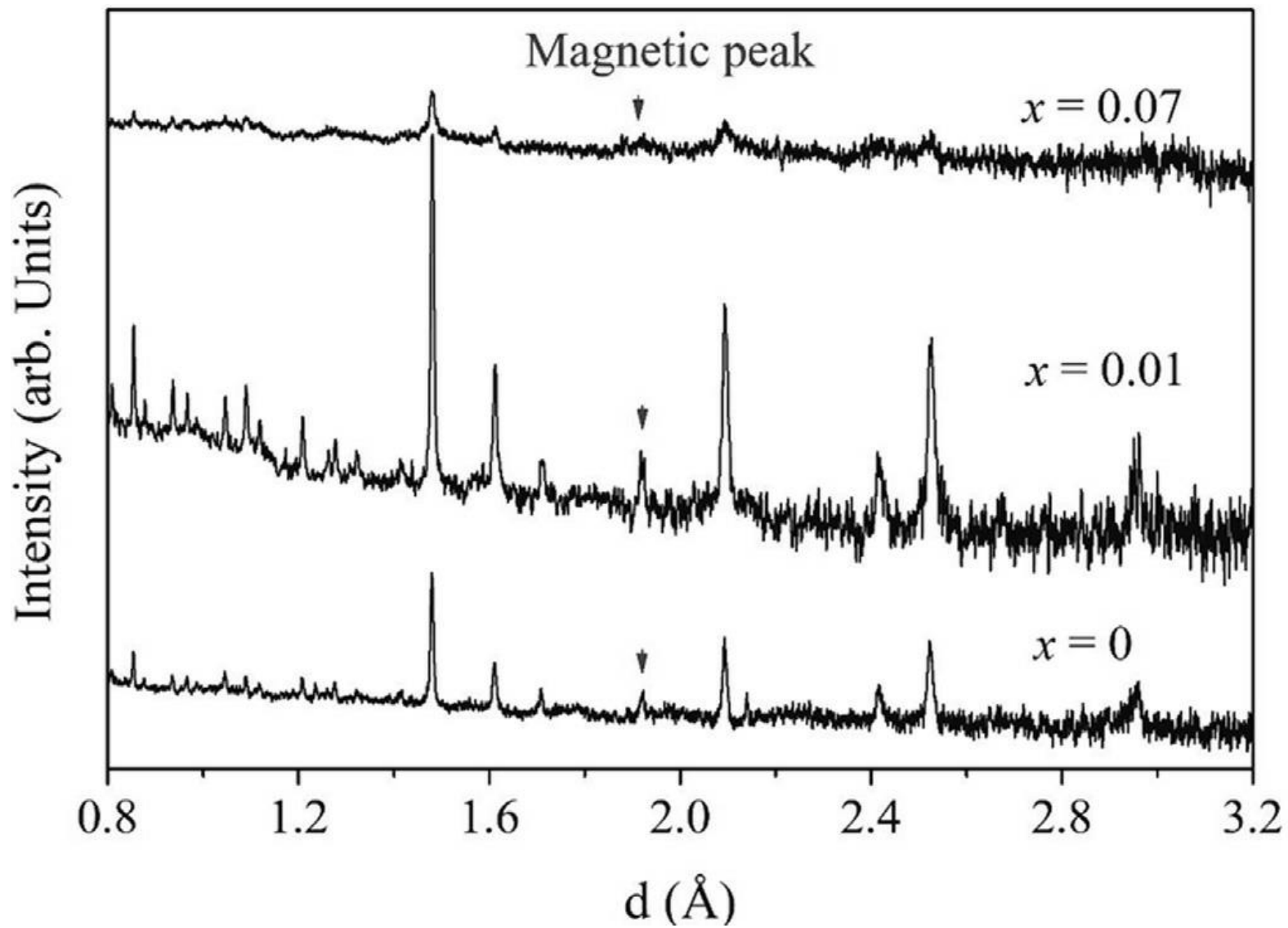


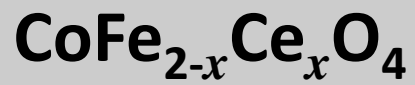
Typical long range ferrimagnetic
order

Finite size effects lead to a reduction in magnetism
and the appearance of superparamagnetic phase
in ultrasmall particles

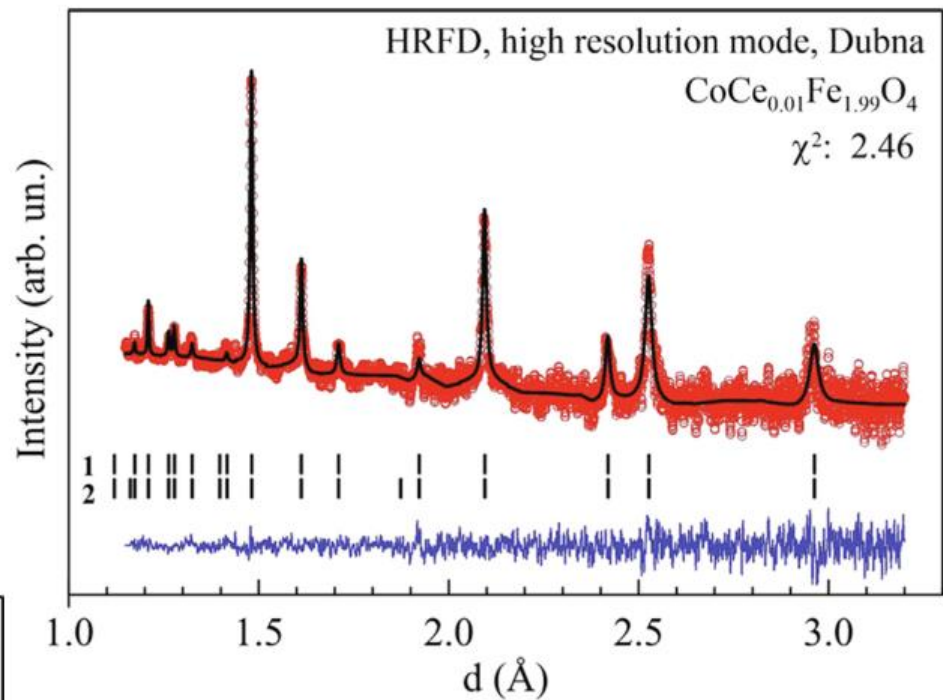
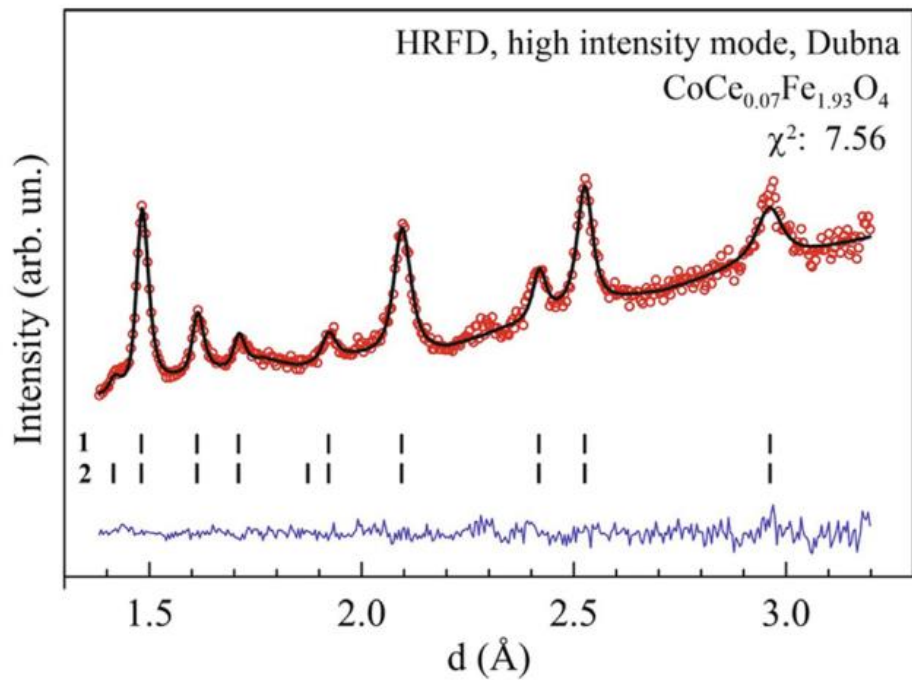


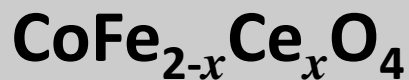
ND





ND





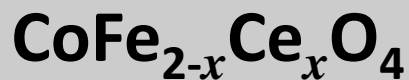
ND

XRD

x	D (nm)	a_{XRD} (Å)	a_{th} (Å)	A-O cal. (Å)	B-O cal. (Å)	u^{3m} (Å)	u^{43m} (Å)
0	57(1.4)	8.358(4)	8.367	1.859	2.064	0.272	0.397
0.01	46(1)	8.369(4)	8.346	1.849	2.062	0.273	0.398
0.03	39(0.7)	8.364(5)	8.348	1.846	2.064	0.273	0.398
0.05	22(0.3)	8.385(6)	8.33	1.836	2.064	0.274	0.399
0.07	21(0.3)	8.377(7)	8.321	1.829	2.064	0.274	0.399
0.1	21(0.4)	8.374(8)	8.328	1.826	2.068	0.274	0.399

Neutron Diff.

Parameter	$x = 0.0$	$x = 0.01$	$x = 0.07$
a_{cub} , Å	8.375	8.380	8.378
x (O)	0.249(1)	0.256(1)	0.252(1)
$n_{\text{(A)}}$ (Fe)	0.99(8)	0.95(9)	0.97(9)
$\mu_{\text{(A)}}/\mu_{\text{(B)}}$, μ_{B}	5.9/3.94(12)	5.9/2.68(13)	5.9/2.95(17)
A-O, Å	1.807(5)	1.900(3)	1.84(1)
B-O, Å	2.097(5)	2.047(3)	2.08(1)
L, Å	767	530	274



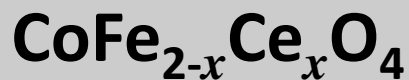
ND

XRD

x	D (nm)	a_{XRD} (Å)	a_{th} (Å)	A-O cal. (Å)	B-O cal. (Å)	u^{3m} (Å)	u^{43m} (Å)
0	57(1.4)	8.358(4)	8.367	1.859	2.064	0.272	0.397
0.01	46(1)	8.369(4)	8.346	1.849	2.062	0.273	0.398
0.03	39(0.7)	8.364(5)	8.348	1.846	2.064	0.273	0.398
0.05	22(0.3)	8.385(6)	8.33	1.836	2.064	0.274	0.399
0.07	21(0.3)	8.377(7)	8.321	1.829	2.064	0.274	0.399
0.1	21(0.4)	8.374(8)	8.328	1.826	2.068	0.274	0.399

Neutron Diff.

Parameter	$x = 0.0$	$x = 0.01$	$x = 0.07$
a_{cub} , Å	8.375	8.380	8.378
x (O)	0.249(1)	0.256(1)	0.252(1)
$n_{(\text{A})}$ (Fe)	0.99(8)	0.95(9)	0.97(9)
$\mu_{(\text{A})}/\mu_{(\text{B})}$, μ_{B}	5.9/3.94(12)	5.9/2.68(13)	5.9/2.95(17)
A-O, Å	1.807(5)	1.900(3)	1.84(1)
B-O, Å	2.097(5)	2.047(3)	2.08(1)
L, Å	767	530	274



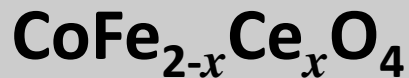
ND

XRD

x	D (nm)	a_{XRD} (Å)	a_{th} (Å)	A-O cal. (Å)	B-O cal. (Å)	u^{3m} (Å)	u^{43m} (Å)
0	57(1.4)	8.358(4)	8.367	1.859	2.064	0.272	0.397
0.01	46(1)	8.369(4)	8.346	1.849	2.062	0.273	0.398
0.03	39(0.7)	8.364(5)	8.348	1.846	2.064	0.273	0.398
0.05	22(0.3)	8.385(6)	8.33	1.836	2.064	0.274	0.399
0.07	21(0.3)	8.377(7)	8.321	1.829	2.064	0.274	0.399
0.1	21(0.4)	8.374(8)	8.328	1.826	2.068	0.274	0.399

Neutron Diff.

Parameter	$x = 0.0$	$x = 0.01$	$x = 0.07$
a_{cub} , Å	8.375	8.380	8.378
x (O)	0.249(1)	0.256(1)	0.252(1)
$n_{\text{(A)}}$ (Fe)	0.99(8)	0.95(9)	0.97(9)
$\mu_{\text{(A)}}/\mu_{\text{(B)}}$, μ_{B}	5.9/3.94(12)	5.9/2.68(13)	5.9/2.95(17)
A-O, Å	1.807(5)	1.900(3)	1.84(1)
B-O, Å	2.097(5)	2.047(3)	2.08(1)
L, Å	767	530	274



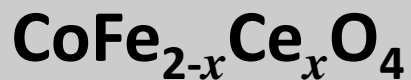
ND

XRD

x	D (nm)	a_{XRD} (Å)	a_{th} (Å)	A-O cal. (Å)	B-O cal. (Å)	u^{3m} (Å)	u^{43m} (Å)
0	57(1.4)	8.358(4)	8.367	1.859	2.064	0.272	0.397
0.01	46(1)	8.369(4)	8.346	1.849	2.062	0.273	0.398
0.03	39(0.7)	8.364(5)	8.348	1.846	2.064	0.273	0.398
0.05	22(0.3)	8.385(6)	8.33	1.836	2.064	0.274	0.399
0.07	21(0.3)	8.377(7)	8.321	1.829	2.064	0.274	0.399
0.1	21(0.4)	8.374(8)	8.328	1.826	2.068	0.274	0.399

Neutron Diff.

Parameter	$x = 0.0$	$x = 0.01$	$x = 0.07$
a_{cub} , Å	8.375	8.380	8.378
x (O)	0.249(1)	0.256(1)	0.252(1)
$n_{\text{(A)}}$ (Fe)	0.99(8)	0.95(9)	0.97(9)
$\mu_{\text{(A)}}/\mu_{\text{(B)}}$, μ_{B}	5.9/3.94(12)	5.9/2.68(13)	5.9/2.95(17)
A-O, Å	1.807(5)	1.900(3)	1.84(1)
B-O, Å	2.097(5)	2.047(3)	2.08(1)
L, Å	767	530	274



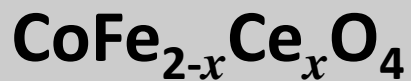
ND

XRD

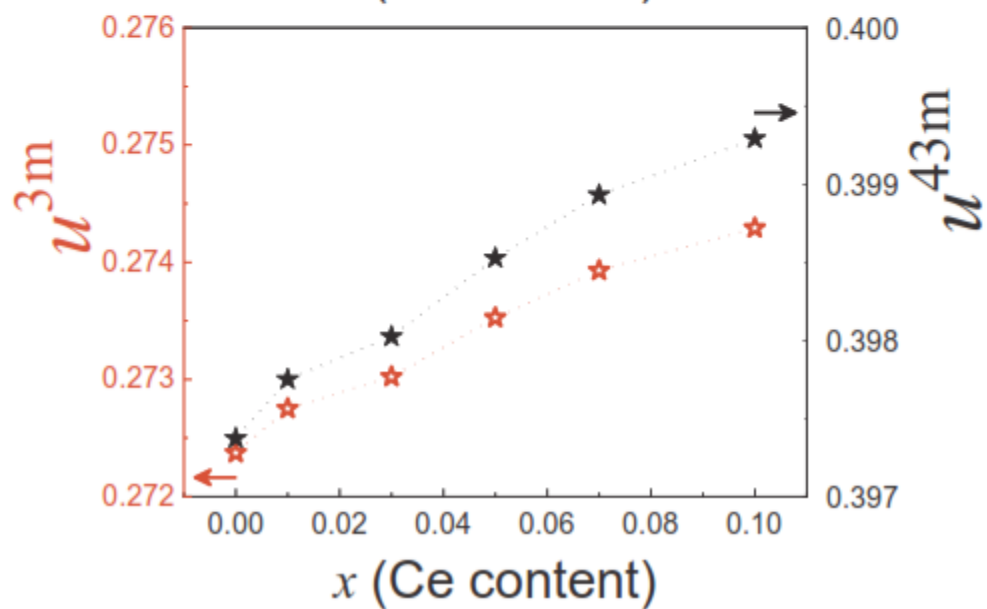
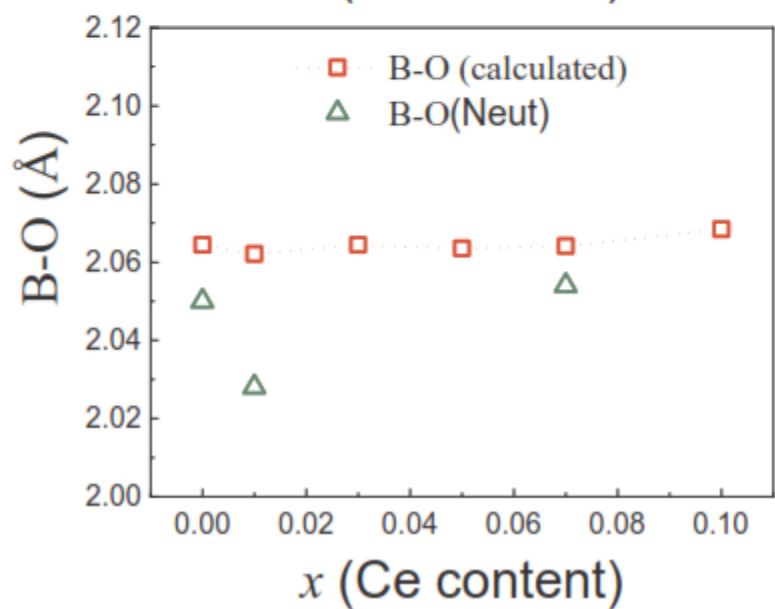
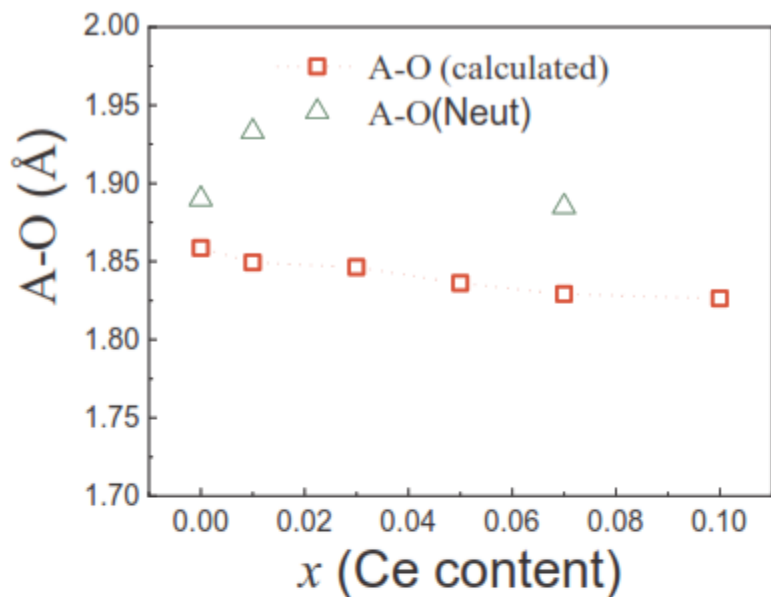
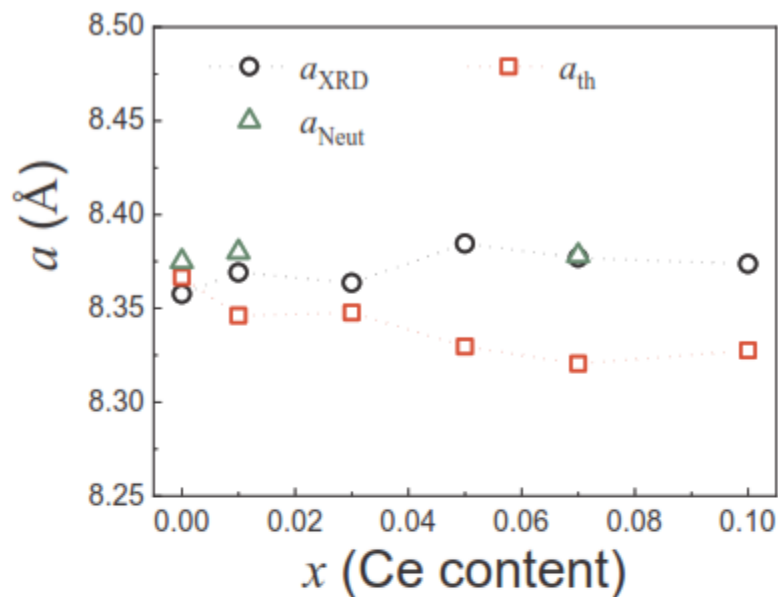
x	D (nm)	a_{XRD} (Å)	a_{th} (Å)	A-O cal. (Å)	B-O cal. (Å)	u^{3m} (Å)	u^{43m} (Å)
0	57(1.4)	8.358(4)	8.367	1.859	2.064	0.272	0.397
0.01	46(1)	8.369(4)	8.346	1.849	2.062	0.273	0.398
0.03	39(0.7)	8.364(5)	8.348	1.846	2.064	0.273	0.398
0.05	22(0.3)	8.385(6)	8.33	1.836	2.064	0.274	0.399
0.07	21(0.3)	8.377(7)	8.321	1.829	2.064	0.274	0.399
0.1	21(0.4)	8.374(8)	8.328	1.826	2.068	0.274	0.399

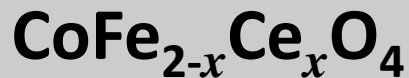
Neutron Diff.

Parameter	$x = 0.0$	$x = 0.01$	$x = 0.07$
a_{cub} , Å	8.375	8.380	8.378
x (O)	0.249(1)	0.256(1)	0.252(1)
$n_{(\text{A})}$ (Fe)	0.99(8)	0.95(9)	0.97(9)
$\mu_{(\text{A})}/\mu_{(\text{B})}$, μ_{B}	5.9/3.94(12)	5.9/2.68(13)	5.9/2.95(17)
A-O, Å	1.807(5)	1.900(3)	1.84(1)
B-O, Å	2.097(5)	2.047(3)	2.08(1)
L, Å	767	530	274



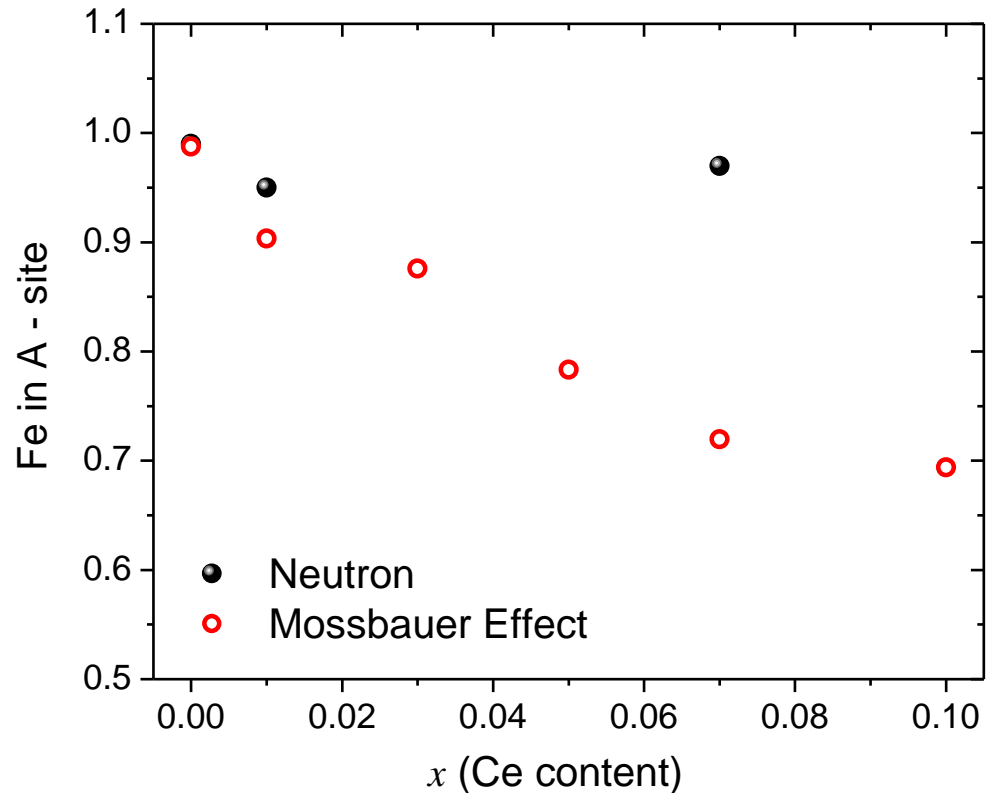
ND





ND

x	Cation Distribution (Mössbauer Effect)	Cation Distribution (Neutron Diffraction)	δ Mössbauer Effect	δ Neutron Diffraction
0	(Fe _{0.988} Co _{0.012}) [Fe _{1.012} Co _{0.988}]O ₄	(Fe _{0.99} Co _{0.01}) [Fe _{1.01} Co _{0.99}]O ₄	0.988	0.99
0.01	(Fe _{0.903} Co _{0.097}) [Fe _{1.087} Co _{0.903} Ce _{0.01}]O ₄	(Fe _{0.95} Co _{0.05}) [Fe _{1.04} Co _{0.95} Ce _{0.01}]O ₄	0.903	0.95
0.03	(Fe _{0.876} Co _{0.124}) [Fe _{1.094} Co _{0.876} Ce _{0.03}]O ₄		0.876	
0.05	(Fe _{0.783} Co _{0.217}) [Fe _{1.167} Co _{0.783} Ce _{0.05}]O ₄		0.783	
0.07	(Fe _{0.72} Co _{0.28}) [Fe _{1.21} Co _{0.72} Ce _{0.07}]O ₄	(Fe _{0.97} Co _{0.03}) [Fe _{0.96} Co _{0.97} Ce _{0.07}]O ₄	0.72	0.97
0.1	(Fe _{0.694} Co _{0.306}) [Fe _{1.206} Co _{0.694} Ce _{0.1}]O ₄		0.694	



Conclusion

- **Ce³⁺ doping decreases the particle size of the prepared samples.**
- **TEM measurements confirm the formation of nano sized – spherical shaped particles.**
- **XRD illustrates a single spinel phase for all the prepared samples and a gradual decrease of D with increasing Ce content was observed.**
- **VSM measurements spot a gradual decrease in the saturation magnetization with decreasing D.**
- **Mössbauer effect spectroscopy suggests the coexistence of the magnetic order for large particle sizes and superparamagnetic behavior for ultrasmall particles.**
- **Neutron diffraction measurements capture the reduced particle size and the magnetic order.**

Thanks for your attention!